We thank both the anonymous reviewer and Zhibo Zhang for their careful reading of the manuscript and their useful suggestions. We respond to each of the reviewer's comments and criticisms below:-

Anonymous Referee #1

Received and published: 2 April 2020

This manuscript compares satellite retrievals of above-cloud aerosol optical properties and underlying cloud properties with aircraft measurements over the South-East Atlantic during the CLARIFY-2017 field campaign. The main novelty of this work is the performance and limitations of aerosol and cloud properties from SEVIRI with aircraft data. This manuscript is well-written and is suitable for publication in ACP after ad dressing the comments. Please note the page and line number in my comments are based on version 1 of the manuscript, which can be found in the supplement.

We would like to thanks the reviewer for a careful review. We are glad that the reviewer found the work novel, and are pleased that they find the manuscript well-written. We have taken the reviewers comments into account is what follows:

Specific Comments:

P4 line 4-7: The filtering criteria for SEVIRI is used to remove non-opaque and inhomogeneous clouds. However, the discussion/conclusion section of this manuscript also mentions that algorithmic assumptions and technical limitations result in aerosol and cloud retrieval errors. Likewise, the Meyer MODIS retrieval also accounts for the uncertainty of retrieval errors. Is it possible for an opaque and homogenous cloud field to be removed simply due to falsely large AOT retrieval differences within a 0.1° grid?

In the review of Part 1, we have shown that the SEVIRI filters were efficient in removing the cloud edge effect. See the figure below where magenta corresponds to pixel removed by of the filter:

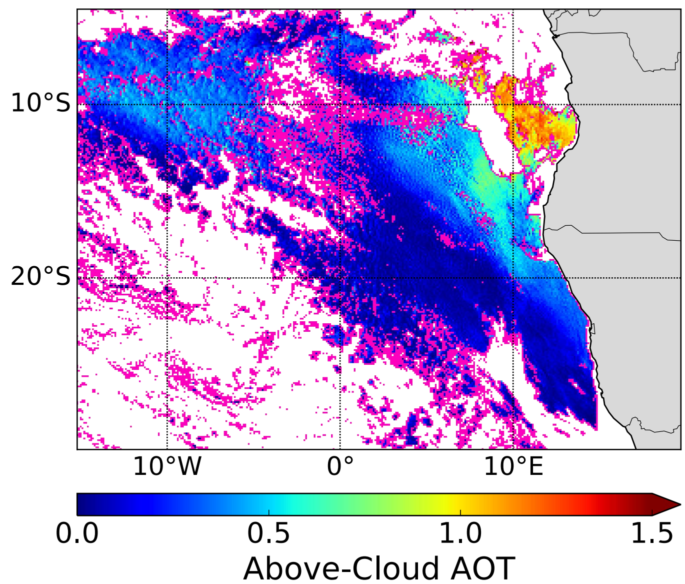

Figure R1: Above cloud AOT at 550 nm retrieved from SEVIRI measurements on the 28 August 2017 at 10:12 UTC over the SEAO. Pixels in magenta correspond to pixels removed with the cloud edge and cloud heterogeneity filters.

Theoretically, a homogeneous cloud field could be removed if the standard deviation of the AOT within the grid cell is too large, but one can see from the plot above that the filters tend to remove scenes close to the cloud edges in a coherent manner. However, what we are trying to achieve with our algorithm is a best estimate of the above sky direct radiative effect from SEVIRI that can be compared to e.g. modelled DRE effects from climate models. Such climate models typically have resolutions of ~100km at these latitudes and they tend to include 2-stream radiative transfer calculations which do not represent the effects of cloud inhomogeneities explicitly. Thus, we believe that it is reasonable to remove cloud edge effects.

For the MODIS retrieval, the filter on the AOT uncertainty is only applied to the AOT product.

P5 line 1-2: Which type of correlation coefficient is this? Sayer et al. (2019) indicated that Spearman's rank correlation coefficient is less sensitive to extreme outliers. Also, I suggest including the root mean square error in all of your scatterplots so that readers can have a better sense of your linear fit performance.

In both the text and the figures, we are using Pearson's correlation coefficients which measure the performance of the linear fits shown in the figure. The Spearman's correlation coefficient assesses how well the relationship between two dataset can be described using a monotonic function, whether linear or not. Consequently, we found that the Pearson's correlation coefficient is more appropriate here (now specified in the text and in the caption of the figures) and that the RMSE would be redundant.

P9 line 4-14: The use of atmospheric profiles from the NWP forecast model for retrievals is unique and is more representative to the realistic atmospheric conditions compared to the *tropical atmospheric profile in McClatchey. However, the tropical atmosphere is only one of several atmospheric profiles in the McClatchey database and is likely the least representative profile compared to mid-latitude summer, mid-latitude winter, sub-arctic summer, and sub-arctic winter profiles over the South-East Atlantic. Each of these four atmospheric profiles has less than 70% of column water vapor in the tropical profiles, so they would be closer to the dropsonde measurements. This paper will be significantly strengthened if the authors can determine the McClatchey profile/s that best represent the southeast Atlantic during the study period even if none of the profiles would perfectly agree with the dropsonde. Thus, I suggest the authors investigate and discuss the atmospheric profiles of the other four profiles.*

We are somewhat surprised by this comment. We are not focusing on a global retrieval. From the Figures in the manuscript (and that included above), the main area of interest is the equatorial Atlantic (Equator – 30°S). Using other McClatchey profiles such sub-Arctic summer and winter are not relevant as they are designed for latitudes of 50°-70°. A widely-accepted definition of mid-latitudes is from the tropics of Cancer/Capricorn polewards to the Arctic circles (south of 23.5°S for our area of interest). If one had to choose a single atmospheric profile for the modelling of irradiances, one would therefore definitely choose the tropical profile.

The reviewer should also keep in mind that the retrievals will only be sensitive to the column water vapour above the cloud. Yes – for the McClatchey mid-latitude summer, there is a reduction of water vapour over the tropical profile, but this is around 75% when summed from 3km-10km.

Our analysis has already incorporated retrievals of water vapour from the NWP model owing to the high degree of variability of water vapour in the atmospheric profile in this region. To start investigating the impact of inferior, non-temporally-varying water vapour profiles beyond with a single McClatchey profile would be a regressive step and would dilute from the focus and novelty of the research.

P12 line 3-5: Aerosol-cloud interactions involve the competing effects of semi-direct and indirect effects, so absorbing aerosols could even enhance cloud albedos. The authors need to provide a reference to support the statement. Alternatively, they need to broaden their arguments to different possibilities of cloud albedo change due to absorbing aerosols.

These sentences have been rephrased:

"Pollution within clouds tends to increase the cloud albedo by acting as cloud condensation nuclei but can also increase their absorption coefficient (Twomey, 1977). Although the brightening of the clouds is typically the dominant effect, the presence of absorbing smoke within the cloud could have an impact on the spectral variation of the cloud reflectance. Both the SEVIRI and the MODIS algorithms assume that the entire aerosol layer is located above an unpolluted cloud and do not account for aerosols within the cloud. Therefore, a reduction in the cloud albedo in the visible/SWIR range due to pollution within the cloud layer could be interpreted by colour-ratio based retrievals as an additional aerosol signal, leading to an overestimation of the above-cloud AOT."

Technical comments:

P2 line 33-36: spell out all the acronyms

Done

P2 line 40: Replace "between" with "among"

Done

P2 line 48: Sayer et al. (2019) also retrieved ACAOT from VIIRS

Done

P3 line 10: "observation of every"

We have kept "With an observation every 15 minutes …".

P3 line 11: what is MSG?

Done

P3 line 28: "SWIR" should have appeared in line 7

Done

P3 line 33: "platform" is unnecessary

Done

P3 line 37: "MODIS uses six channels, which"

Done

P4 line 5: "measurements of cloud edges....."

The sentence has been modified.

P4 line 11: Are optical thicknesses referred to 0.55µm using spectral AOT after the colour-ratio retrieval or before retrieval?

We are not quite sure what the reviewer is referring to here. We state "*Throughout this study, intrinsic optical parameters and derived extrinsic properties such as optical thickness refer to values at an optical wavelength of 0.55 µm.*" We believe that this is sufficiently clear.

P4 line 7: "sensors" seems to be a more suitable word than "methods"

Done

P4 line 18: "slot on the"

Done

P4 line 29: "correlation" should be accompanied by correlation coefficients. A visual agreement is not the same as a strong correlation.

Done

P4 line 33: ". . .by about 1.5μm" – is this based on an average over the entire map?

Modified: *"However, the CER retrieved by SEVIRI are smaller than the MODIS CER by 2 μm on average over the map."*

P4 line 43: "days of observations"

Done

P5 line 9: "has a large impact"

Modified

P5 line 30: "there are more"

Done

P5 line 38: The values 0.937 and -1.460 do not match Figure 3d

Corrected

P6 line 16: "clouds become thicker"

Done

P6 line 38: "outlined the same"

Done

P7 line 11: "are used to remove"

Done

P7 line 41: "over the ocean"

Done

P7 line 50: What is "FASTEM"?

Added: "*the fast ocean emissivity model FASTEM*"

P7 line 50: Liu et al. (2011) is not in the reference list. However, Liu et al (2010a,b) are present. Please clarify the references.

Done (Liu et al, 2010)

P9 line 14: Remove "against"

Done

P9 line 26: "show that the"

Done

P9 line 26: "layer. However, no evidence"

Done

P10 line 6: It appears that the sign changes at about 2.7˚E rather than 4˚W

Corrected

P10 line 6: "After" is a confusing word. I suggest "From the west of"

Done

P10 line 24: "maneuvers"

We have kept manoeuvres as the rest of the paper is in British English.

P10 line 43-46: Is the standard deviation of the satellite retrievals based on only one group of 60km radius comparisons between satellite and aircraft measurements during each flight day?

The standard deviation is calculated for each flight with the all the AOT retrieved within the 60km radius. The sentence has been modified to:

"*... the error bars correspond to the standard deviation calculated for each flight of the MODIS and SEVIRI AOT retrieved within the 60 km radius.*"

P11 line 10: Is there a correlation coefficient or only an agreement?

It is an agreement. The sentence has been modified:

"This could explain why a better agreement is obtained between the in situ measurements and the satellite products on the AAOT than on the AOT for all flights except C044, C048 and C051."

P11 line 20-24: It is unclear about the type of data filtering that has been applied in this section. Was the inhomogeneity parameter applied in this section to remove low cloud fraction area? Are Meyer's retrieval uncertainties applied?

The satellite data filtering used in section 3 is similar to section 2. In the first paragraph of section 2.a, the following sentence has been added:

"Note that those filters have been applied to the satellite data used in both the section 2 and 3."

P11 line 29 – P12 line 5: This paragraph is disconnected from the rest of the section. It should either be a part of the cloud layer section (d. ii.) or a sub section of c.

The aim of this paragraph is to illustrate the impact of aerosols within clouds on the satellite retrieval of the AOT above clouds. For these reason, we prefer to keep this paragraph in the section about the aerosol layer. The following sentence has been added at the beginning of the paragraph:

"Information on the vertical profile of aerosols can be used to further investigate the differences between satellite observations and in situ measurements."

P12 line 22: "CDP is less than"

Done

P12 line 29: "In Figure 9c"

Done

P12 line 47: "useful in enhancing"

Done

P13 line 38-39: "is shown in Figure 10"

Done

P15 line 11: "significantly enhance"

Done

Figure 2: The figure label "cloud AOT" appears to be one word.

Done

Figure 3: The grey dash line is not explained in the figure caption and is very unclear in the printed version. I suggest changing the dashed line to black for clarity.

Done

Figure 6: The word "Longitude" is partially missing in the label of the horizontal axis

Done

Figure 8: There are 2 points on the CER=13 micron. Are those the maximum values?

These are the largest values of the data in these plots.

Figure 10: Describe panel a, b and c in the figure caption

Done

Table 3: "SEVIRI (no aerosol)"

Done

Zhibo Zhang (Referee)

zhibo.zhang@umbc.edu **Received and published: 3 April 2020**

This is the second part of a remote sensing study of the above cloud smoke aerosols in the South East Atlantic Ocean (SEAO) region based on the observation from the SE- VIRI satellite sensor. The first part documents the theoretical basis of the retrieval algorithm and relevant technical details. In this part, the SEVIRI retrievals results are evaluated first through comparisons with an independent satellite retrieval product based on MODIS observations. Then the retrievals are further compared with collocated in situ measurements from the recent CLARIFY-2017 field campaign. Overall, the SEVIRI based above-cloud aerosol (ACA) retrievals are in reasonable agreement with MODIS ACA retrievals and direct in situ measurements. The differences among each retrieval products are studied, and the potential reasons causing the differences are provided.

This paper is a useful addition to the studies on the ACA in the SEAO region. Because of its location and geostationary nature, the SEVIRI observations are ideal for studying the ACA and the underlying clouds, even though the algorithm used here is not really new and has been developed/applied in several previous studies. The manuscript is well organized and easy to read. Overall it is good shape. However, I have several questions and some major concerns regarding the methodology used in the comparisons, which should be explained and clarified before it can be accepted for publications. In addition, I have some thoughts about the differences between SEVIRI and other measurements/retrievals that are different from the paper. I would like to share them and hopefully, them can be helpful for improving the paper.

We would like to thank Zhibo Zhang for his useful and insightful review. He is right that the algorithm is not entirely new; however the spectral band differences and the geostationary nature of the satellite platform mean that SEVIRI does have some potentially unique capabilities for e.g. examining the diurnal cycle of ACI etc. We are glad that the reviewer finds the paper well organised, easy to read and in overall good shape. We have taken account of the reviewer's comments in what follows:

Questions/Comments/Suggestions:

1. Overall, the references cited in the Introduction and other parts of the manuscripts are rather old. A number of recent studies on the ACA in the SEAO region should be referenced here. For example, there are several recent studies on the direct radiative effects of ACA in SEAO region e.g., [Wilcox, 2012; Zhang et al., 2016b; Kacenelenbogen et al., 2019] should be cited here at line 26 when discussing the DRE of ACA. They are more relevant than Keil and Haywood (2003) in this context. When discussing the CALIPSO ACA retrievals, the three cited studies are based on the two-way transmittance method by Hu et al. (2007). But the operational CALIPSO Aerosol retrieval product, which is based on the "traditional" lidar ratio method, is much more widely used. It should be mentioned with reference here.

We have updated the reference in the introduction by adding the following text:

"These new observations have been used in recent satellite-based studies on the direct radiative effect of aerosols above clouds in the SEAO (Wilcox et al., 2012; Peers et al., 2015; Zhang et al., 2016b; de Graaf et al., 2019; Kacenelenbogen et al., 2019). However, validation exercises are needed to evaluate the accuracy of these new methodologies."

"De Graaf et al. (2020) have compared the direct radiative effect of aerosols above clouds obtained from SCIAMACHY, OMI/MODIS and POLDER and have shown that differences can be expected from instruments with different spatial resolution due to 3D effects of clouds."

> *2. I have several major concerns and comments about how the SEVIRI retrievals are compared with the MODIS retrievals in Section 2. They need to be clarified and some comparisons should be repeated if possible.*
>
> *a. Spatial collocation and data screening: as pointed in the paper, the two instruments have a significantly different spatial resolution, SEVIRI at 3x3km at nadir and MODIS at 1x1km. So roughly there are 9 MODIS pixels within each SEVIRI pixel. In this study, both retrievals are aggregated to 0.1o x0.1o common grid box (∼10km). I understand that pixel-to-pixel collocation between SEVIRI and MODIS may be challenging. BTW, it is not a bad idea to explain to the readers why pixel-to-pixel collocation is difficult. But I believe there must be some quality assurance measures to filter out some "bad" or challenging grid boxes that are not suitable for comparison. For example, some 0.1o x0.1o grid boxes may be partly cloudy and others can have either bad SEVIRI or MODIS ACA retrievals. What are the conditions used here to filter out these "bad" grid boxes? If they are not filtered, what are the considerations to keep them and what are the potential implications of the ACA comparison results?*

The SEVIRI filters for partly cloudy observations, cloud edges and heterogeneous clouds are based on the observations aggregated onto the 0.1° × 0.1° grid. At pixel level, the MODIS algorithm uses the Partly Cloudy Pixel detection algorithm from the operational MOD06 cloud retrieval. In addition to those criteria, the observations not suitable for the comparison are rejected using the uncertainty on the retrieved AOT for MODIS and the quality of the fit for SEVIRI as described in section 2.a.

The following two sentences of text have been added to section 2.a:

"Cloud edges, fractional cloud coverage and heterogeneous clouds are also rejected from the SEVIRI results using observations aggregated at a 0.1° × 0.1° grid resolution."

"Comparisons at the native resolution of the instruments is challenging notably because of the rapid evolution and advection of the clouds."

In section 2.b.ii, we have introduced an additional filter on the CER to take into account the fact that the MODIS retrieval is limited to CER<30 µm:

"In addition to the filters described in section 2.a, observations associated with CER_{SEVIRI} *> 30 µm are removed to be consistent with the upper limit of the MODIS retrieval."*

b. Sanity check on "clean" clouds: in my opinion, it is really difficult to understand the ACA retrieval difference between SEVIRI and MODIS without first understanding their differences for "clean" clouds (i.e., not aerosols above). For example, in Figure 3 there is some significant difference between the SEVIRI, and MODIS retrieved COT and CER. It is hard to tell whether these differences are caused by the ACA correction or something in the cloud retrieval part. To address this question, I'd strongly recommend a comparison of the COT and CER between the two satellite sensors for "clean" clouds, even only for some case studies.

Cloud properties from MODIS and SEVIRI have been compared for low above-cloud AOT (<0.05) and the results are shown in the figure below.

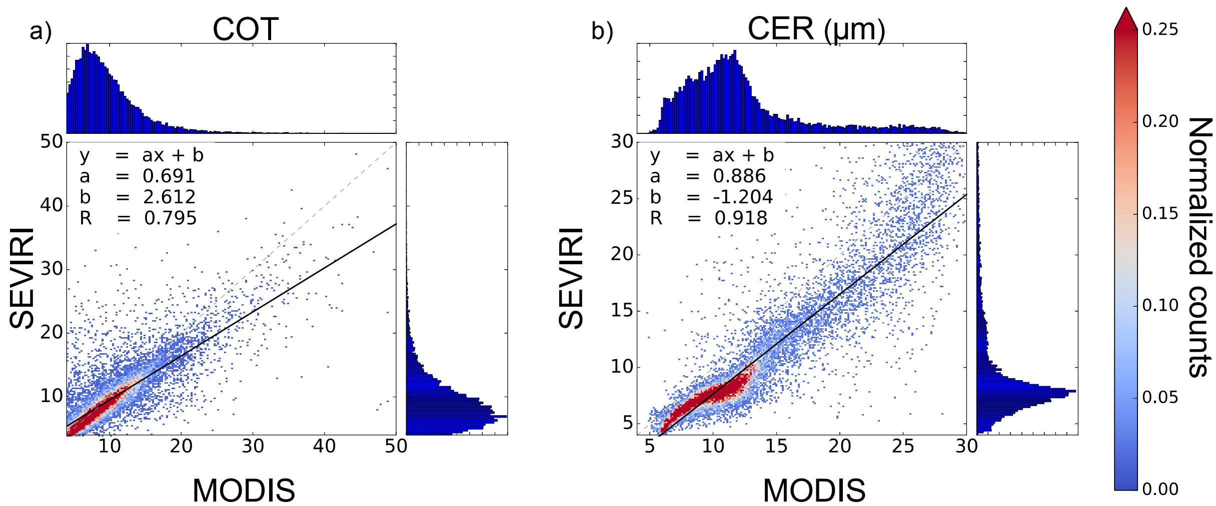

Figure R2: Scatterplots and data distributions for the comparison of the COT (a) and the CER (b) retrieved when the above-cloud AOT is lower than 0.05 by SEVIRI and MODIS (MOD06ACAERO) between the 28th August and 5th September 2017 over the area between 0˚N - 30˚S and 20˚W - 15˚E. The black lines represent the linear regression.

Note that the filter on the MODIS AOT uncertainty has been omitted for this analysis. The differences between the relationships observed with and without aerosols above clouds are small and could be related to the smaller size of the dataset. This confirms that the differences between the cloud properties from MODIS and SEVIRI mainly come from the assumptions in the cloud retrieval and the differences between the two instruments. The following text has been added at the end of section 2.b.ii:

"Note that the cloud properties from SEVIRI and MODIS have also been compared for low above-cloud AOT (AOT < 0.05) to separate the impact of the aerosol correction from the cloud retrieval itself. The Figure S1 in the supplement shows that similar relationships are obtained with and without aerosols above clouds."

c. The sampling rate of SEVIRI ACA retrieval needs to be analyzed and reported, and the implications explained. The SEVIRI sampling strategy is "The SEVIRI algorithm rejects both the aerosol and cloud products when the COT is lower than 3". Based on Figure 1 and Figure 2, it seems that this strategy would lead to a significant loss of samples. Note that, as pointed out in Zhang et al. (2016) the dramatic difference in sampling rate is an important reason for the fact that the DREs of ACA in the SEAO region reported in the literature differ so substantially. In fact, based on the combination of CALIOP and MODIS, Zhang et al. (2016) found that a large fraction of the ACA cases has COT smaller than 3 (See Figure 9a) of Zhang et al. (2016). The authors need to estimate the fraction of the ACA cases they sample vs. how many they filtered out. Moreover, it should be explained how this sampling strategy could impact the user of the data, for example, when calculating the DRE of ACA.

Using the operational SEVIRI cloud property retrieval from the Met Office (Saunders et al., 2006), we have estimated that the fraction of low level clouds associated with COT lower than 3 is 15.5% for the observation of the 4th September 2017 at 10:15 UTC. While we agree that removing these pixels is not ideal when comparing to GCM models, a 10 x 10 km resolution is getting close to the resolution limit for operational global NWP models that can examine the impacts of clouds. Thus, by clearly stating our assumptions, we argue that the same screening procedure can be applied to the models as applied to the SEVIRI algorithm when making an objective comparison. In the CLARIFY-2017 overview paper (Haywood et al., 2020), Figure R3 shows the above-cloud DARE comparison between POLDER and HadGEM. Note that all COTs lower than 3 from HadGEM were removed in order to be consistent with the satellite screening. This analysis has shown that the direct radiative effect from biomass burning aerosols is relatively independent of the resolution for GCMs.

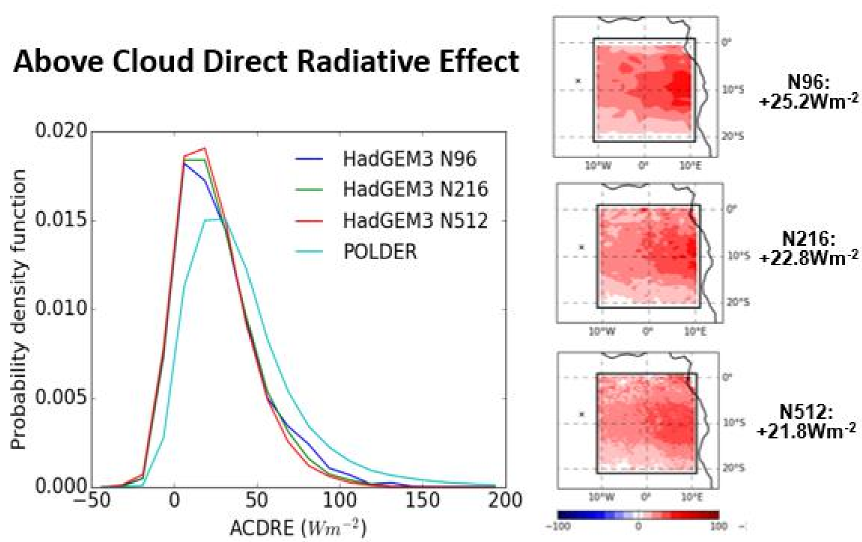

Figure R3: Above cloud direct radiative effect diagnosed from the Unified model (N96, N216 and N512 resolution) over the area shown in the panels in the right-hand column. The probability density function of the above cloud direct radiative effect is also shown from POLDER after (Peers et al., 2016). The intercomparison is for August-September 2006 and model data is matched to instantaneous POLDER retrievals. (From Haywood et al., 2020.)

The following statement has been added at the end of section 2.b.i:

"This difference in the cloud sampling between the two methods can lead to a significant difference when comparing the regional mean of the above-cloud direct radiative effect (Zhang et al., 2016). However, the 0.1° × 0.1° grid resolution used here is close to the typical resolution of global operational numerical weather prediction models that can examine the impact of clouds. Therefore, when comparing to global climate models (e.g. as per the model/POLDER comparison detailed in Haywood et al., 2020), users are advised to use a similar screening procedure to the satellite retrieval."

> *d. Uncertainty analysis is needed in the comparison: I didn't find any error bar associated either SEVIRI or MODIS retrievals. The signal to noise ratio for ACA retrieval is not very large. So, the uncertainty associated with either retrieval is considerably large. The comparison is only meaningful when they are put in the context of their error budget. Otherwise, the comparison may very well be comparing statistic noises. In particular, I'd suggest adding an error budget to both products in Figure 3. You may put the AOT into several bins and plot the uncertainty of AOT retrievals from each product as an error bar (x-axis error bar for MODIS and y for SEVIRI). Then, the differences between the two products need to be put in the context of the error budget.*

We agree. In Peers et al. (2019), the uncertainty on the AOT retrieved by SEVIRI due to the aerosol, the cloud model, the Rayleigh scattering (i.e. the altitude of the aerosol and the cloud layer) and the water vapour correction have been estimated to be 40%, 0.3%, 2.5% and 10% respectively. The uncertainty due to the measurements has been estimated by calculating the standard deviation of the SEVIRI AOT in Figure 3 for each AOT bin. The total uncertainty is obtained by combining the uncertainties listed above, assuming that they are independent (i.e. using the square root of the sum of squares). The MODIS uncertainty, which is provided by the algorithm, accounts for the Rayleigh scattering errors, the measurement errors and the errors due to the aerosol and the cloud model. The error bars have been added to Figure 3. The following text has been added to section 2.b.ii:

"The error bars in Figure 3a represent the uncertainty associated with the retrieved AOT. In Peers et al. (2019), the uncertainty of the AOT retrieved by SEVIRI due to the aerosol, the cloud model, the Rayleigh scattering (i.e. the altitude of the aerosol and the cloud layer) and the water vapour correction have been estimated to be 40%, 0.3%, 2.5% and 10% respectively. The uncertainty due to the measurements has been estimated by calculating the standard deviation of the SEVIRI AOT in Figure 3a for each AOT bin. The total uncertainty is obtained by combining the uncertainties listed above, assuming they are independent (i.e. using the square root of the sum of squares). The MODIS uncertainty, which is provided by the algorithm, accounts for the above-cloud column two-way transmittance errors, the Rayleigh scattering errors, the measurement errors and the errors due to the aerosol and the cloud model. As with SEVIRI, the aerosol model assumption is typically the largest source of uncertainty in the MODIS retrieval (Meyer et al., 2015)."

> *e. The explanation for the differences between SEVIRI and MODIS ACA and cloud retrievals in Figure 3 is not very convincing. There are a number of differences between the SEVIRI and MODIS ACA retrievals in Figure 3. First of all, AOT from the SEVIRI*

retrieval is significantly smaller than MODIS results by about 20%. The paper attributes this mainly to the difference in the aerosol model assumed in the two schemes, e.g., the aerosol model in the SEVIRI retrieval is more absorptive than that in the MODIS retrieval. But this explanation is not very convincing. The SSA difference between the two is only 0.01 (0.85 in SEVIRI vs. 0.86 in MODIS). This is equivalent of about 6% difference in absorption AOT (i.e., 0.01/0.15), which can only explain half of the ~11% difference between SEVIRI and MODIS AAOT in table 1. To provide a more convincing explanation, I'd suggest the authors run the SEIVIRI ACA retrievals using the same aerosol model as MODIS and then make comparisons. Secondly, the correlation between SEIVIRI and MODIS retrieval is clearly nonlinear. The authors are aware of this nonlinearity and pointed it out in the paper. However, no explanation is provided. BTW, the correlation between the two AAOT retrievals in Figure 3 b is also nonlinear. I wouldn't say this is "slightly". It is clearly and significantly nonlinear. In my opinion, this nonlinearity is partly, if not mainly, due to the sampling difference between the two retrieval algorithms, i.e., MODIS screens out retrievals based on retrieval uncertainty while SEIVIR keeps low-quality retrievals which are mainly low AOT. This goes back to my earlier comments on the sampling differences. Some quality assurance screening is clearly needed here.

In response to the reviewer's comments, the SEVIRI retrieval has been run using both the CLARIFY-2017 and the MOD06ACAERO aerosol model for the case study shown in Figure 2 in the manuscript, i.e. the 4th September 2017 at 10:15 and 11:45 UTC. Figures R4 below shows the comparison between MODIS and SEVIRI for the above cloud AOT. The slope of the regression line between SEVIRI and MODIS goes from 0.81 with the CLARIFY-2017 model to 1.05 with the MOD06ACAERO model. Moreover, the mean AOT for this case study is 0.44 for MODIS, 0.33 for SEVIRI using the CLARIFY-2017 model and 0.44 for SEVIRI using the MOD06ACAERO model. This confirms that, for AOT larger than 0.25, the differences between the SEVIRI and the MODIS retrieval are mainly due to the assumed aerosol properties.

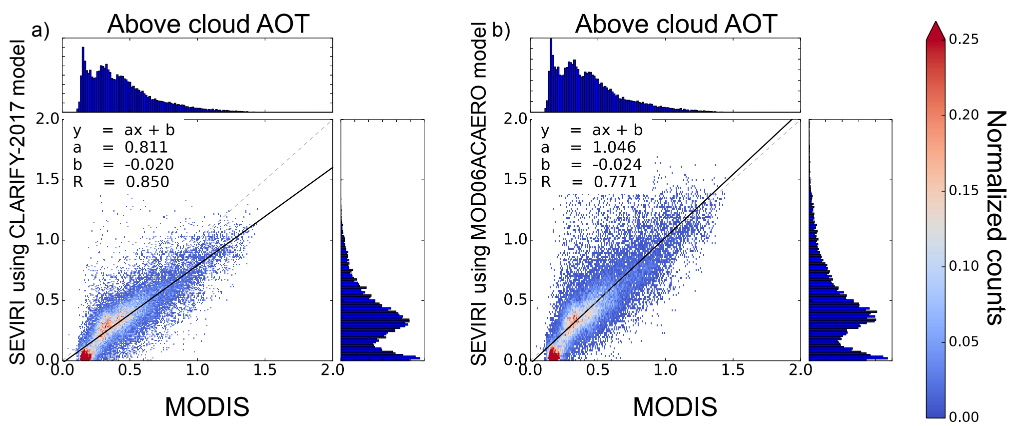

Figure R4: Comparison of the above-cloud AOT retrieved by SEVIRI and MODIS (MOD06ACAERO) in the morning of the 4th September 2017 over the area between 0˚N - 30˚S and 20˚W - 15˚E. The left plot (a) corresponds to the SEVIRI retrieval using the CLARIFY-2017 aerosol model and the right plot (b) shows the SEVIRI retrieval using the same aerosol model as the MODIS retrieval. The black lines represent the linear regression.

The non-linearity of the correlation between the SEVIRI and the MODIS AOT and AAOT is caused by the MODIS filter on the uncertainty and, to a lesser extent, by the AOT dependence of the MOD06ACAERO model. The correlation obtained when the uncertainty filter is not applied is shown in Figure R5 below.

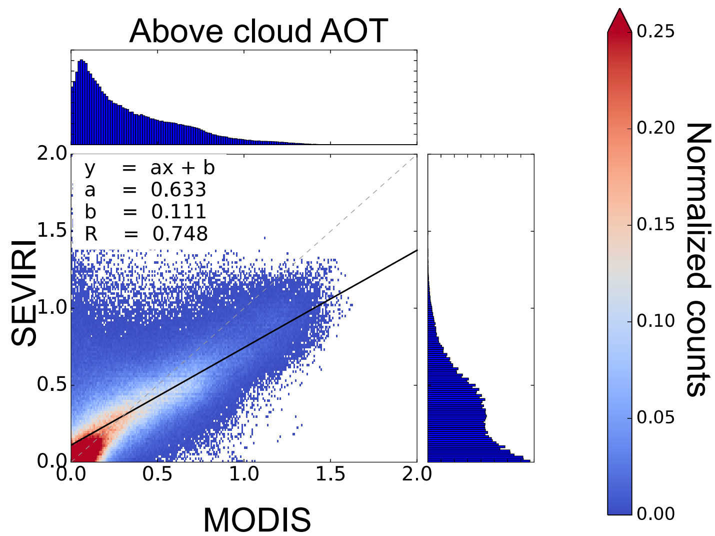

Figure R5: Comparison of the above-cloud AOT from SEVIRI and MODIS (MOD06ACAERO) retrieved between the 28^{th} August and 5^{th} September 2017 over the area between 0˚N - 30˚S and 20˚W - 15˚E. The filter on the MODIS uncertainty has not been applied.

Indeed, the signal to noise ratio is smaller for small AOT, leading to a larger fractional uncertainty. For the MODIS dataset, users are advised to consider that AOT=0 when the uncertainty is larger than 100%. Although no filters are applied to remove those results in the SEVIRI dataset, we expect their contribution to the total DRE over the South East Atlantic to be small. We have made a rough estimate of the above-cloud DRE using the AOT from the dataset used in section 2.b.ii and a COT of 11 and a CER of 8µm, which are close to the median values observed by SEVIRI (see Table 1 in the paper). Based on radiative transfer calculations performed with the CLARIFY-2017 aerosol model, a DRE by AOT of $109.65 W.m^{-2}. \tau^{-1}$ has been obtained. Figure R6 below shows the cumulative contribution to the total DRE as a function of the above-cloud AOT. The total DRE is $36.1 W.m^{-2}$ using SEVIRI, with the AOT below 0.1 contributing to less than $1.2 W.m^{-2}$. Finally, when comparing to GCM, it is possible to exclude the low AOT from both the satellite observations and the models.

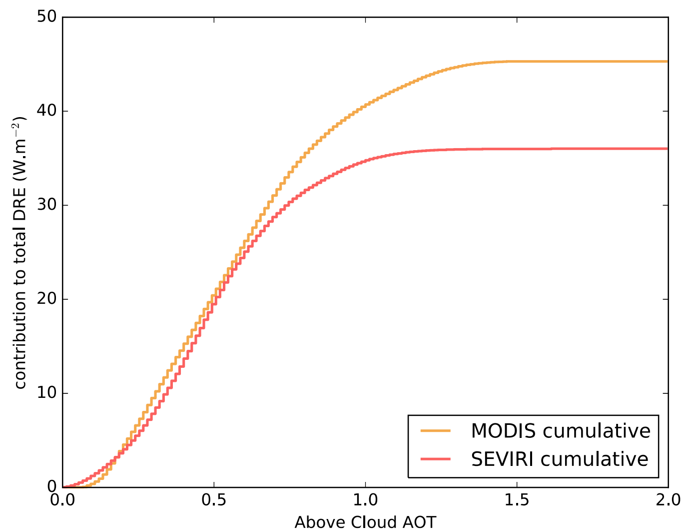

Figure R6: Cumulative contribution to the total above-cloud DRE as a function of the AOT for the dataset used in section 2.b.ii, considering a COT of 11 and a CER of 8µm.

This section has been modified to:

"To assess the impact of the aerosol assumptions on the retrieved AOT, the SEVIRI retrieval has been run using both the CLARIFY-2017 and the MOD06ACAERO aerosol model for the case study described in section 2.b.i. The comparison of the both sets of AOT with MODIS is plotted in Figure 4. The slope of the regression line between SEVIRI and MODIS is 0.81 with the CLARIFY-2017 model and it is 1.05 when the same model (i.e. MOD06ACAERO model) is used. Moreover, the mean AOT for this case study is 0.44 for MODIS, 0.33 for SEVIRI using the CLARIFY-2017 model and 0.44 for SEVIRI using the MOD06ACAERO model. This confirms that, for AOT larger than 0.25, the differences between the SEVIRI and the MODIS retrieval are mainly due to the assumed aerosol properties. While the CLARIFY-2017 and ORACLES observations provide a thorough and comprehensive analysis of the BBA optical properties, which are adopted by the SEVIRI and MODIS satellite retrievals, representing the level of complexity of the variation of optical properties owing to evolution of flaming to smouldering combustion during the biomass burning season (Eck et al., 2003) and the complexity of aerosol ageing processes (e.g. Wu et al, 2020; Taylor et al., 2020) is beyond current observational capabilities. The non-linearity of the AOT and AAOT comparison as well as the differences between the SEVIRI and MODIS distributions at low values can be partly explained by the MODIS filter on the AOT uncertainty. The signal to noise ratio being smaller at low AOT, the near zero AOT_{MODIS} are typically associated with an uncertainty larger than 100% and are discarded. Although no filters are applied to remove those results in the SEVIRI dataset, their contribution to the total DRE over the South-East Atlantic are expected to be small."

3. At line 25 of page 6, when discussing the plane-parallel bias, there are few much more recent studies that should be noted here, in particular [Zhang et al., 2016a] proposed a 2-D framework to account for the plane-parallel bias in both COT and CER retrievals caused by sub-pixel inhomogeneity.

The reference has been added.

4. In Figure 6, to what extent the longitudinal variation of delta_AAOT is caused by the variation of AAOT itself? It seems to me that the percentage difference is mainly determined by the denominator, i.e., the mean value of the AAOT. I'd suggest adding the climatological domain averaged AAOT to Figure 6 as a reference.

For this figure, we have selected AAOT > 0.03, which corresponds to $AOT_{SEVIRI}>0.2$, to minimize the effect of the denominator on the AAOT variation. The AAOT from SEVIRI and MODIS used to calculate ΔAAOT have been added to Figure 6.

5. At line 1 of page 13, can the authors explain why the aerosol absorption and its wavelength dependence have anything to do with the Twomey effect?

These sentences have been rephrased:

"Pollution within clouds tends to increase the albedo of clouds by acting as cloud condensation nuclei but can also increase their absorption coefficient (Twomey, 1977). Although the brightening of the clouds is typically the dominant effect, the presence of absorbing smoke within the cloud could have an impact on the spectral variation of the cloud reflectance. Both the SEVIRI and the MODIS algorithms assume that the entire aerosol layer is located above an unpolluted cloud and do not account for aerosols within the cloud. Therefore, a reduction in the cloud albedo in the visible/SWIR range due to pollution within the cloud layer could be interpreted by colour-ratio based retrievals as an additional aerosol signal, leading to an overestimation of the above-cloud AOT."

6. At line 22 of page 22, there are actually several more recent studies that suggest the CER retrievals are overestimated when there is significant sub-pixel cloud inhomogeneity [Zhang and Platnick, 2011; Zhang et al., 2012; 2016a].

The references have been added.

References Kacenelenbogen, M. S. et al. (2019), Estimations of global shortwave direct aerosol radiative effects above opaque water clouds using a combination of A-Train satellite sensors, Atmospheric Chemistry and Physics, 19(7), 4933–4962, doi:10.5194/acp-19-4933-2019.

Wilcox, E. M. (2012), Direct and semi-direct radiative forcing of smoke aerosols over clouds, Atmospheric Chemistry and Physics, 12(1), 139–149, doi:10.5194/acp-12-139-2012.

Zhang, Z., A. S. Ackerman, G. Feingold, S. Platnick, R. Pincus, and H. Xue (2012), Effects of cloud horizontal inhomogeneity and drizzle on remote sensing of cloud droplet effective radius: Case studies based on large-eddy simulations, J Geophys Res, 117(D19), D19208–, doi:10.1029/2012JD017655.

Zhang, Z., and S. Platnick (2011), An assessment of differences between cloud effec- tive particle radius retrievals for marine water clouds from three MODIS spectral bands, J Geophys Res, 116(D20), D20215, doi:10.1029/2011JD016216.

Zhang, Z., F. Werner, H. M. Cho, G. Wind, S. Platnick, A. S. Ackerman, L. Di Girolamo, A. Marshak, and K. Meyer (2016a), A framework based on 2-D Taylor expansion for quantifying the impacts of sub-pixel reflectance variance and covariance on cloud optical thickness and effective radius retrievals based on the bi-spectral method, Journal of Geophysical Research-Atmospheres, 2016JD024837, doi:10.1002/2016JD024837.

Zhang, Z., K. Meyer, H. Yu, S. Platnick, P. Colarco, Z. Liu, and L. Oreopoulos (2016b), Shortwave direct radiative effects of above-cloud aerosols over global oceans derived from 8 years of CALIOP and MODIS observations, ACP, 16(5), 2877–2900, doi:10.5194/acpd-15-26357-2015.

Eck, T. F., Holben, B. N., Ward, D. E., Mukelabai, M. M., Dubovik, O., Smirnov, A., Schafer, J. S., Hsu, N. C., Piketh, S. J., Queface, A., Roux, J. L., Swap, R. J., and Slutsker, I.: Variability of biomass burning aerosol optical characteristics in southern Africa during the SAFARI 2000 dry season campaign and a comparison of single scattering albedo estimates from radiometric measurements, J. Geophys. Res.-Atmos., 108, 8477, https://doi.org/10.1029/2002JD002321, 2003.

Saunders, R.W., R.A. Francis, P.N. Francis, J. Crawford, A.J. Smith, I.D. Brown, R.B.E. Taylor, M. Forsythe, M. Doutriaux-Boucher and S.C. Millington, 2006. The exploitation of Meteosat Second Generation Data in the Met Office. Proceedings of the 2006 EUMETSAT Meteorological Satellite Conference, Helsinki, Finland.

Taylor, J. W., Wu, H., Szpek, K., Bower, K., Crawford, I., Flynn, M. J., Williams, P. I., Dorsey, J., Langridge, J. M., Cotterell, M. I., Fox, C., Davies, N. W., Haywood, J. M., and Coe, H.: Absorption closure in highly aged biomass burning smoke, Atmos. Chem. Phys., 20, 11201–11221, https://doi.org/10.5194/acp-20-11201-2020, 2020.

Wu, H., Taylor, J. W., Szpek, K., Langridge, J., Williams, P. I., Flynn, M., Allan, J. D., Abel, S. J., Pitt, J., Cotterell, M. I., Fox, C., Davies, N. W., Haywood, J., and Coe, H.: Vertical variability of the properties of highly aged biomass burning aerosol transported over the southeast Atlantic during CLARIFY-2017, Atmos. Chem. Phys. Discuss., https://doi.org/10.5194/acp-2020-197, in review, 2020.

We thank the editor, Paquita Zuidema, for her careful reading and constructive suggestions for our manuscript. Below, we have addressed her questions and comments and indicated the changes in the manuscript:

> *The authors have done an excellent job of addressing the concerns of the two reviewers and I do not feel they need to be asked to re-review. As editor, I am motivated to make an additional comment on the MARSS-SEVIRI LWP comparison shown in Fig 11 and discussed on p. 16. I'm surprised to see the authors rely solely on an assumption of a LWC profile that is constant with height (their eqn 2) when many papers now point to the more realistic applicability of an adiabatic profile. Painemal and Zuidema 2011, which they cite, is just one of many examples and indeed they mention applying a linearly-increasing LWC with height on line 14, p. 19. This would change the factor 2/3 to a factor of 5/9 in eqn 2, further reducing the SEVIRI-retrieved LWP and increasing the discrepancy from the MARSS values.*

To reflect the adiabatic nature of the cloud formation, we have modified equation 2 in the manuscript and use 5/9 instead of 2/3:

"Considering an adiabatic cloud, the LWP from SEVIRI is derived from the retrieved COT and CER using the following relationship:

$$LWP_{SEVIRI} = \frac{5}{9}\rho_l \times COT \times CER \qquad (2)$$

where ρ_l is the density of liquid water. It should be noted that the effective radius at the cloud top is expected to be slightly larger than the CER retrieved by SEVRI because of penetration depth effects (Platnick, 2000), which could lead to a small underestimation of the LWP from SEVIRI."

Figures S7 in the supplement and 11 in the manuscript have been changed accordingly.

> *Given that the effective radii retrievals match reasonably well in Fig. 10, another explanation for the LWP difference might be in the MARSS LWP. There is no error analysis included within the description of the MARSS data and we do not know its retrieved LWP uncertainty. Larger drizzle/precipitation sized drops will increase the microwave emission beyond that expected by the microwave retrieval algorithm - the authors don't say, but I suspect the algorithm assumes Rayleigh scattering. The C050 comparison, for which the drop sizes are the largest in Fig. 10, could be an example of that. C042, in which the MARSS and SEVIRI LWPs match fairly well until about 10:15 (which actually serves to support both retrievals, up to that point), breaks down thereafter, and precipitation could explain this, as it would also reduce the visible optical depth. I am not sure why an ref comparison is not included in Fig. 10 for C042 - was the CDP not working for this flight? I note that Seethala and Horvath, 2010, 10.1029/2009JD012662, use a threshold of 180 g/m^2 to distinguish when precipitation starts impacting satellite microwave LWP retrievals, and the MARSS instrument operates at higher frequencies than the satellites, with the MARSS frequencies more susceptible to enhancement of the brightness temperature by rain (there's also some relevant discussion in Grosvenor et al., 2018, 10.1029/2017RG000593 p 435-436, containing other references).*

The following paragraph has been added at the end of section 3.a.ii:

"Errors in the MARSS LWP retrievals arise from several sources, including errors in the forward model used in the retrieval, the instrument noise and calibration errors. Instrument noise and calibration errors are estimated to be less than 1K, and the combined instrument and forward-model error in the retrieval is assumed to be uncorrelated with a standard deviation of 2K. The overall uncertainty in the retrieved LWP is estimated by combining the posterior error covariance from the retrieval with sensitivity estimates derived by perturbing fixed input parameters such as the sea surface temperature, wind speed, cloud top and base heights, and water vapour profile within plausible ranges. The total uncertainty is estimated to be approximately 40 g m^{-2} at low LWP (< 200 g m^{-2}) and it increases with increasing LWP becoming about 10-12% at large LWP (> 400 g m^{-2})."

As pointed out by the editor, the retrieval assumes Rayleigh scattering. It also makes the further assumption that the cloud droplets are purely absorbing, and neglects scattering effects. To assess the impact of larger cloud drops on the LWP retrieval, simulations have been performed using full Mie scattering optical properties for cloud droplets, considering a 1 km thick cloud with constant liquid water content, and a similar particle size distribution to the SEVIRI retrievals. The plots below show the impact of the effective radius on the simulated brightness temperatures for 3 values of LWP at the two frequencies used. The left-hand column shows the brightness temperatures, and the right-hand column shows the difference between the full-scattering calculation and the "Rayleigh-absorption-only" assumption used in the retrieval. For the largest CDP-derived CER in the manuscript (~15 μm) the difference is less than 0.1K. For a CER of 48 μm, which is amongst the largest values observed during CLARIFY-2017, the error is less than 0.2K. For these reasons, we do not think that the discrepancies between the SEVIRI and the MARSS LWP come from the cloud drop size.

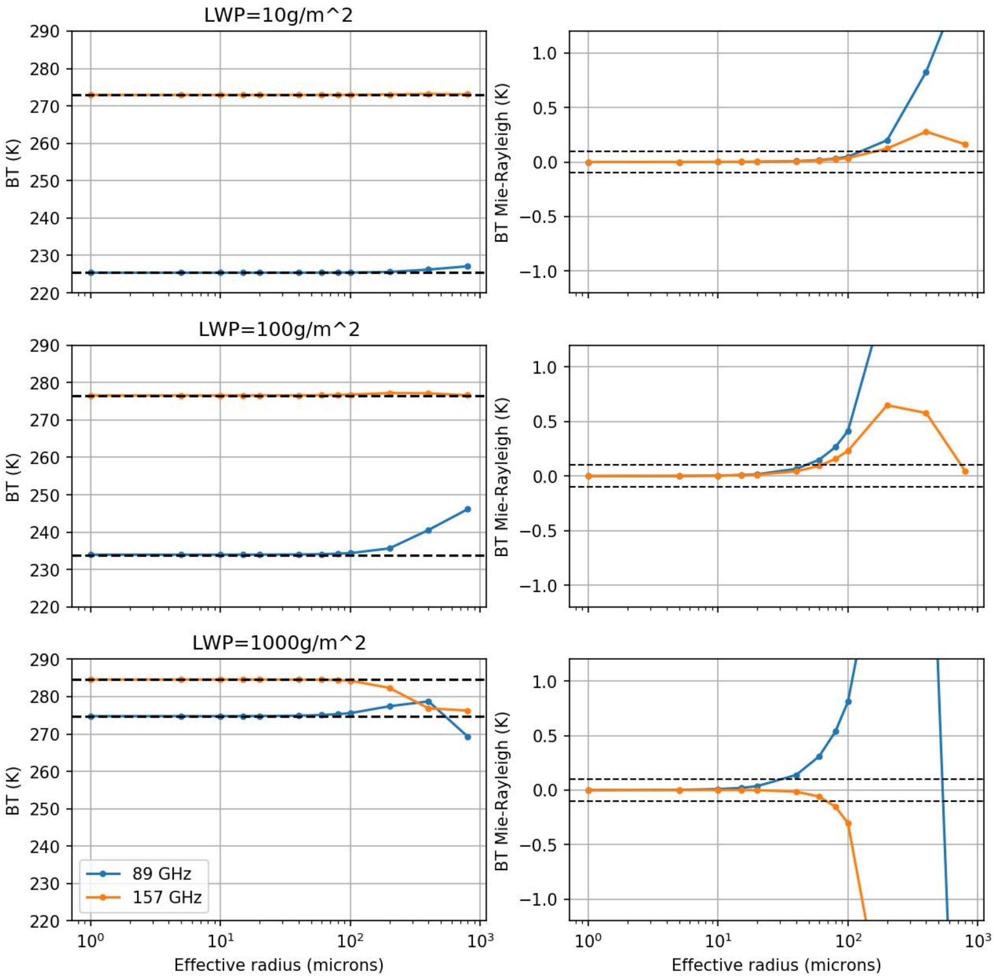

Figure 1: Impact of the cloud droplet effective radius on the Brightness Temperature (BT) at the frequencies used to retrieve the LWP from MARSS.

For precipitating cases, the MARSS retrieval makes no distinction between cloud liquid and precipitation, and returns the total liquid water path. However, it still makes the "Rayleigh-absorption-only" assumption, even for precipitation. Simulations have been performed to determine the likely errors induced by this assumption by performing further full-scattering calculations as follows. In this case, the cloud liquid is assumed to be uniform between 1000 and 1500 m, with a LWP of 400 g m^{-2}. The precipitation is assumed to be uniform between 0 and 1500 m and the rain water content is adjusted to give different values of total water content (i.e. cloud and rain). The cloud effective radius is assumed to be 20 µm (effective variance of 0.077), and the rain effective radius is assumed to be 100 µm (effective variance of 0.3). The plot below compares the full scattering simulations (coloured lines) with the Rayleigh-absorption-only simulations (dashed lines, left-hand plot). The right hand plot shows the difference between the two, which indicates that non-Rayleigh and scattering effects are still only ~1K even at the highest values of total water path, and are therefore reasonably accounted for already in the forward model uncertainty estimate.

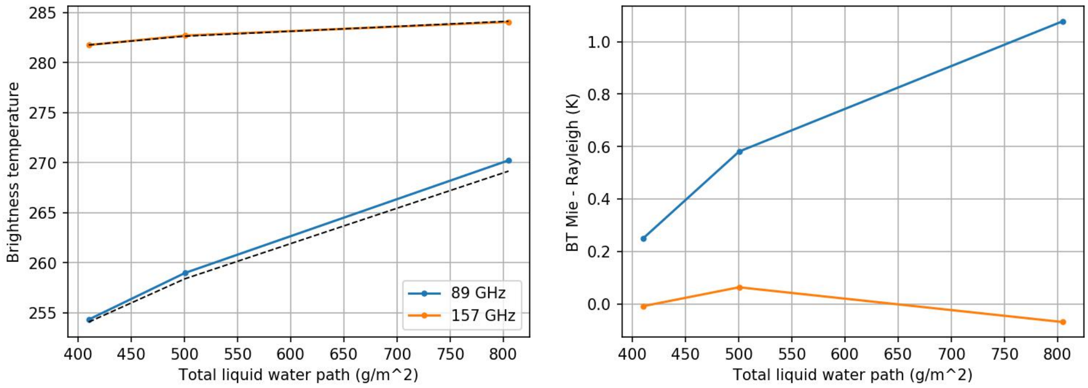

Figure 2: Evolution of the brightness temperature at MARSS frequencies as function of the total liquid water path (i.e. cloud and precipitation) using full scattering simulations (coloured lines, left plot) and Rayleigh-absorption-only simulations (dashed lines, left plot) and difference between the two simulations (right plot).

On the other hand, the LWP obtained from SEVIRI does not account for precipitation. The following text has been added to section 3.d.ii:

"It is also important to add that the MARSS retrieval makes no distinction between cloud liquid and precipitation, and returns the total liquid water path. On the other hand, the LWP obtained from SEVIRI does not account for precipitation. Therefore, the LWP from MARSS is expected to be larger than SEVIRI in the presence of rain and drizzle drops."

"Moreover, the peaks of LWP from MARSS and the overall larger values than SEVIRI could also be attributed to the contribution of drizzle and precipitation which is not accounted for in the LWP derived from the satellite. In-flight visual observations report drizzle during the 3 flights and droplets with an effective radius larger than 100 µm were detected by a 2 Dimensional Stereo probe during C049 and C050. There is no clear evidence of precipitation in the measurements from the vertical profiles but it is difficult to completely discount this type of local precipitation events during the long runs above cloud top that were performed with MARSS."

The reason for the missing C042 plot in the CDP comparison figure (Figure 10 in the manuscript) is that no SLR has been performed within the cloud during that flight.

> *Another cause for the discrepancy could be that the SEVIRI-retrieved cloud top effective radius for the two-layer cumulus-under-stratocumulus regime that dominates the cloud field at Ascension (some examples are shown in the cited Abel et al., 2020; others overlapping with the CLARIFY time period are also shown in Zhang and Zuidema, 2019, ACP SI), is not representative of the column, with the upper stratiform layer consisting of smaller drops than the lower-lying cumulus. The authors could use the aircraft data to test for this; it also seems suggested by Fig. 9.*

For the 3 flights analysed in section 3.d.ii, the cloud regime consisted of stratoculumus above shallow cumulus. The CDP measurements from the vertical profiles indicate that the shallow cumulus layer consisted of smaller droplets than the upper stratocumulus. The following sentences have been added at the beginning of the section:

"The dominant cloud regime around Ascension Island typically consists of a stratocumulus layer above shallow cumulus (Zhang and Zuidema, 2019). For the flights selected here, the CDP measurements from the vertical profiles indicate that the shallow cumulus layer consisted of smaller droplets than the upper stratocumulus and that the liquid water content increases with height."

> *The LWP comparison is summarized on p. 18, line 11 as revealing a limitation to the COT retrieval (the upper limit), but I am not sure that that is what is going on here.I would like to ask the authors to discuss whether or not precipitation may be unrealistically enhancing the MARSS LWPs - is there data from ascent/descent profiles that could be used to look for precip? The ref/LWC profile? And to revisit the relevant text in their manuscript based on the considerations raised above.*

The following sentences have been added to the conclusion:

"Although the variations of the satellite LWP follows those of the aircraft observations, the LWP obtained from SEVIRI is typically smaller than the measurements from MARSS. The drizzle observed during these flights partly explain this discrepancy as the LWP from SEVIRI does not account for drizzle and rain while the MARSS instrument does. An underestimation of the LWP due to an underestimation of the COT by SEVIRI can also be expected in case of extremely large LWP (i.e. > 600 $g.m^{-2}$) because the algorithm is limited to a COT of 80."

> *A small further comment is to revisit the reference list and update where appropriate; the Wu paper is now published for example.*

The references to Wu et al. (2020) and Redemann et al (2019) have been updated.

Observation of absorbing aerosols above clouds over the South-East Atlantic Ocean from the geostationary satellite SEVIRI - Part 2: Comparison with MODIS and aircraft measurements from the CLARIFY-2017 field campaign

Fanny Peers[1,2], Peter Francis[23], Steven J. Abel[23], Paul A. Barrett[23], Keith N. Bower[34], Michael I. Cotterell[1,23,45], Ian Crawford[34], Nicholas W. Davies[1,23], Cathryn Fox[23], Stuart Fox[23], Justin M. Langridge[23], Kerry G. Meyer[56], Steven E. Platnick[56], Kate Szpek[23], Jim M. Haywood[1,23]

[1] College of Engineering, Mathematics, and Physical Sciences, University of Exeter, Exeter, UK
[2] Now at: Laboratoire d'Optique Atmosphérique, Université de Lille, Villeneuve d'Ascq, France
[32] Met Office, Fitzroy Road, Exeter, UK
[43] Centre for Atmospheric Science, School of Earth and Environmental Science, University of Manchester, Manchester, UK
[54] Now at: School of Chemistry, University of Bristol, Bristol, UK
[65] NASA GSFC, Maryland, USA.

Correspondence to: F. Peers (fanny.peers@univ-lille.frf.peers@exeter.ac.uk)

Fanny Peers[1], Peter Francis[2], Steven J. Abel[2], Paul A. Barrett[2], Keith N. Bower[3], Michael I. Cotterell[1,2,4], Ian Crawford[3], Nicholas W. Davies[1,2], Cathryn Fox[2], Stuart Fox[2], Justin M. Langridge[2], Kerry G. Meyer[5], Steven E. Platnick[5], Kate Szpek[2], Jim M. Haywood[1,2]

[1] College of Engineering, Mathematics, and Physical Sciences, University of Exeter, Exeter, UK
[2] Met Office, Fitzroy Road, Exeter, UK
[3] Centre for Atmospheric Science, School of Earth and Environmental Science, University of Manchester, Manchester, UK
[4] Now at: School of Chemistry, University of Bristol, Bristol, UK
[5] NASA GSFC, Maryland, USA.

Correspondence to: F. Peers (f.peers@exeter.ac.uk)

Abstract. To evaluate the SEVIRI retrieval for aerosols above clouds presented in Part 1 of the companion paper, the algorithm is applied over the South East Atlantic Ocean during the CLARIFY-2017 field campaign period. The first step of our analysis compares the retrieved aerosol and cloud properties against equivalent products from the MODIS MOD06ACAERO retrieval (Meyer et al., 2015). While the correlation between the two satellite retrievals of the above-cloud Aerosol Optical Thickness (AOT) is good (R=0.785), the AOT retrieved by SEVIRI is 20.316.5% smaller than that obtained from the MODIS retrieval. This difference in AOT is attributed mainly to the more absorbing aerosol model assumed for the SEVIRI retrieval compared to MODIS. The underlying Cloud Optical Thickness (COT) derived from the two satellites are in good agreement (R=0.90). The Cloud droplet Effective Radius (CER) retrieved by SEVIRI is consistently smaller than MODIS by 2.2~2 µm, which is mainly caused by the use of different spectral bands of the satellite instruments. In the second part of our analysis, we compare the forecast water vapour profiles used for the SEVIRI atmospheric correction as well as the aforementioned aerosol and cloud products with in situ measurements made from the Facility for Airborne Atmospheric Measurements (FAAM) aircraft platform during the CLARIFY-2017 campaign. Around Ascension Island, the column water vapour used to correct the SEVIRI signal is overestimated by 3.1 mm in the forecast compared to that measured by dropsondes. However, the evidence suggests that the accuracy of the atmospheric correction improves closer to the African coast. Consistency is observed between the SEVIRI above-cloud AOT and in situ measurements (from cavity ring-down spectroscopy instruments) when the measured single scattering albedo is close to that assumed in the retrieval algorithm. On the other hand, the satellite retrieval overestimates the AOT when the assumed aerosol model is not absorbing enough. Consistency is also found between the cloud properties retrieved by SEVIRI and the CER measured by a cloud droplet probe and the liquid water path derived from a microwave radiometer. Despite the instrumental limitations of the geostationary satellite, the consistency obtained between SEVIRI, MODIS and the aircraft measurements demonstrates the ability of the retrieval in providing additional information on the temporal evolution of the aerosol properties above clouds.

1. Introduction

To accurately predict future climate, it is essential to reduce the uncertainty in the representation of aerosols, clouds and their radiative impacts in climate models (Myhre et al., 2013). Therefore, new in situ and remote sensing strategies are needed to improve our understanding of aerosol-cloud-radiation interactions and to constrain models (Seinfeld et al., 2016). The South East Atlantic Ocean (SEAO) is an ideal region to analyse the effects of partially absorbing aerosols on the radiative budget, the atmospheric stability, clouds and precipitation. The biomass burning aerosols emitted from July to October in southern Africa are mostly transported westward in the residual continental boundary layer in the free troposphere (Abel et al., 202019). These absorbing biomass burning particles are frequently observed above the extensive stratocumulus deck covering the SEAO. For this reason, the region has been the focus of much work over the past few years. Using aircraft and surface-based instrumentation, large scale field campaigns have been deployed in 2016-2018 (Zuidema et al., 2016), within the NASA ORACLES (ObseRvations of Aerosols above CLouds and their intEractionS; Redemann et al., 202019), the US DOE LASIC (Layered Atlantic Smoke Interactions with Clouds; Zuidema et al., 2016), the French AEROCLO-sA (AErosol RadiatiOn and CLouds in Southern Africa; Formenti et al., 2019) and the UK CLARIFY-2017 (CLouds and Aerosol Radiative Impacts and Forcing for Year 2017, Haywood et al., 2020) programs. Airborne in situ instruments, active and passive remote sensing instruments, and radiosondes as well as continuous ground-based measurements have been deployed to characterise biomass burning aerosols, clouds and radiation. In addition to improving our knowledge about aerosol-cloud-radiation interaction processes and constrain numerical weather forecast and climate models, this dataset provides for the first time, direct observations of aerosol-above-clouds for validating emerging satellite retrievals.

Until recently, aerosol retrievals from passive satellites were limited to cloud-free skies and their validation was performed against the widely available datasets from ground-based measurements such as aerosol optical depth from the AERONET (Aerosol Robotic NETwork) sun-photometer network. There has been a growing interest in developing methods to quantify aerosols above clouds from space because absorbing aerosols above cloud have long been recognised to exert a significant, but poorly quantified, positive radiative effect (e.g. Keil and Haywood, 2003). While lidar retrievals of aerosols above cloud have been available for some time from the active CALIOP (Cloud-Aerosol Lidar with Orthogonal Polarization) instrument (Hu et al., 2007; Chand et al., 2008; Liu et al., 2014), retrievals of aerosols from passive instrumentation have also been developed. Studies based on the OMI (Ozone Monitoring Instrument; Torres et al., 2012; de Graaf et al., 2019), SCIAMACHY

(SCanning Imaging Absorption SpectroMeter for Atmospheric CHartographY; de Graaf et al., 2012), MODIS (MODerate resolution Imaging Spectroradiometer; Jethva et al., 2013; Meyer et al., 2015, Sayer et al., 2016) and POLDER (POLarization and Directionality of the Earth's Reflectances; Waquet et al., 2013; Peers et al., 2015) satellite instruments have already demonstrated the potential of retrieving both cloud properties and above-cloud Aerosol Optical Thickness (AOT) from passive sensors or deriving the direct radiative effect of aerosols above clouds. These new observations have been used in recent satellite-based studies on the direct radiative effect of aerosols above clouds in the SEAO region (Wilcox et al., 2012; Peers et al., 2015; Zhang et al., 2016b; de Graaf et al., 2019; Kacenelenbogen et al., 2019). However, validation exercises are needed to evaluate the accuracy of these new methodologies. Intercomparisons of the results from the A-train constellation have been performed to evaluate the consistency amongbetween satellite retrievals (Jethva et al., 2014; Deaconu et al., 2017). De Graaf et al. (2020) have compared the direct radiative effect of aerosols above clouds obtained from SCIAMACHY, OMI/MODIS and POLDER and have shown that differences can be expected from instruments with different spatial resolution due to 3D effects of clouds. Despite independent techniques and/or instruments being compared, this type of analysis cannot be considered as a "true" validation exercise. To provide an independent validation of the above-cloud AOT from the MODIS "colour-ratio" method, Jethva et al. (2016) used airborne measurements from previous aircraft measurement campaigns. However, more direct comparison of aerosol and cloud properties are now possible with the measurements made during the latest field experiments. Data collected during the ORACLES campaign have recently been used to evaluate the above-cloud AOT retrieved by the updated Deep Blue algorithm that is used in aerosol retrievals from the MODIS and the VIIRS (Visible Infrared Imaging Radiometer Suite) instrumentssatellite (Sayer et al., 2019).

In the companion paper (Part 1; Peers et al., 2019), an algorithm to retrieve aerosols above clouds from the geostationary SEVIRI instrument was presented. The first step of the method consists of correcting the SEVIRI-measured reflectances for the large impact of the transmittance of atmospheric gases. This correction uses water vapour concentration profiles from the Met Office Unified Model forecast. Then, the above-cloud AOT, the Cloud Optical Thickness (COT) and the Cloud droplet Effective Radius (CER) are simultaneously retrieved from the spectral dependence of the signal in the visible to Sshort Wwave IinfraRred (SWIR) region; this retrieval method is similar to those used to assess aerosol and cloud properties from OMI and MODIS satellite data. The benefit from using data from the SEVIRI instrument is the high temporal frequency of acquisition. With an observation every 15 minutes, the satellite instrument on board the geostationary platform MSG (Meteosat Second Generation) allows the tracking of the transport of biomass burning plumes above clouds and monitoring of the evolving of the cloud cover (Chang and Christopher, 2016; Seethala et al., 2018). In Section 2 of this paper, the SEVIRI retrieval will be compared against the aerosol and cloud products from the MODIS retrieval developed by Meyer et al. (2015) to assess the consistency of the two retrievals over space and time. Section 3 is dedicated to the validation of the atmospheric correction scheme, in addition to benchmarking the retrieved aerosol and the cloud properties against the in situ measurements made from an aircraft platform during CLARIFY-2017. Section 4 presents a discussion and conclusions.

2. Comparison with MODIS

2.a. Dataset and methodology

The first part of this analysis consists of evaluating the consistency (or lack thereof) between the aerosol and cloud products retrieved from SEVIRI and MODIS. The MODIS MOD06ACAERO algorithm developed by Meyer et al. (2015) relies on the colour-ratio effect to retrieve the above-cloud AOT, the COT and the CER using six channels from the visible to the ~~Short-Wave InfraRed (~~SWIR~~)~~. The measurements are compared with precomputed Look Up Tables (LUT) via an optimal estimation method. The cloud properties are the same as those assumed for the MODIS operational cloud retrieval MOD06 (Platnick et al., 2003) and the aerosol model corresponds to the absorbing model used for the MODIS Dark Target Land Aerosol Product MOD04 (Levy et al., 2009). The retrieval is run for both the Terra and Aqua satellites~~ platforms~~ providing retrievals in the morning and afternoon respectively.

Although the SEVIRI and the MODIS retrieval are based on the same approach, there are inherent differences between the two satellite instruments. For instance, the SEVIRI algorithm uses three spectral bands from 0.64 to 1.64 µm while MODIS uses~~has~~ six channels~~ available~~, which cover a wider range (0.47 to 2.10 µm). The SEVIRI channels are also more affected by absorption from atmospheric gases than the MODIS channels because of their bandwidth and their position in the solar spectrum. Finally, the visible channels of SEVIRI have a sampling distance of 3 km at nadir, as opposed to the 1 km spatial resolution of MODIS. These factors suggest that MODIS retrievals of above-cloud aerosol absorption might be more sensitive and accurate compared to those from SEVIRI. Therefore, it is reasonable to assess the performance of the SEVIRI algorithm by comparing retrieved properties against those from MODIS. Note that, throughout this paper, the subscripts MODIS and SEVIRI refer to the quantity relative to the MOD06ACAERO and the SEVIRI aerosol-above-cloud retrievals respectively.

For both sensor~~method~~s, filters have been implemented to ensure that the measurements have been performed in optimum conditions for the retrieval of aerosol and cloud properties. Firstly, colour-ratio based techniques do not perform well over optically thin clouds as the difficulty in separating the scattering from the clouds and the aerosols increases. Secondly, the forward radiative transfer models used for the retrievals are 1D radiative transfer codes and can become unstable at cloud edges and for inhomogeneous or sub-pixel clouds because the independent pixel approximation is not strictly valid and the plane-parallel bias is not negligible (e.g. Marshak and Davis, 2005). The MODIS algorithm provides pixel-level estimates of the retrieval uncertainty. When the retrieval uncertainty is larger than 100% and/or the COT_{MODIS} is lower than 4, the above-cloud AOT_{MODIS} is rejected. Note that the filter on the AOT uncertainty partly removes the lowest AOTs. Pixels identified as partly cloudy and/or associated with cloud edges are not processed by the MOD06ACAERO retrieval. For SEVIRI, the retrieval is performed for COT_{SEVIRI} larger than 3,~~ and~~ poorly fitted measurements ~~due to cloud edges, inhomogeneous clouds~~ and observations in the glory backscattering region are removed. Cloud edges, fractional cloud coverage and heterogeneous clouds are also rejected from the SEVIRI results using observations aggregated at a 0.1° × 0.1° grid resolution. Readers are referred to Meyer et al. (2015) and Peers et al. (2019) for a complete description of the MODIS and the SEVIRI filters. Note that those filters have been applied to the satellite data used in both the section 2 and 3. Comparisons at the native resolution of the instruments is challenging notably because of the rapid temporal evolution and advection of the clouds. In section 2~~Here~~, the aerosol and cloud properties from both methods are aggregated onto a 0.1° × 0.1° grid. Each MODIS overpass is compared with the closest SEVIRI slot in time, which means that there is never more than 8 minutes between the two satellite observations. Throughout this study, intrinsic optical parameters and derived extrinsic properties such as optical thickness refer to values at an optical wavelength of 0.55 µm.

2.b. Results

2.b.i. Case study

The consistency between the MODIS and SEVIRI retrievals is first assessed for a single case study. The RGB composite of the SEVIRI slot on~~f~~ the 4th September 2017 at 10:15 UTC is shown in Figure 1. The aerosol and cloud properties observed by SEVIRI are presented in Figure 2 together with the MODIS products from the Terra overpasses at 10:00 UTC (east) and 11:40 UTC (west). The spatial distribution of the above-cloud AOT detected by SEVIRI (fig. 2a) is typical of the SEAO during the fire season. A biomass burning plume is observed close to the source, from 13˚S to 30˚S along the African coast. The above-cloud AOT is largest near to Angola, with values up to 1.5. A second plume of moderate intensity ($AOT_{SEVIRI} \approx 0.5$) is detected offshore, around [10˚W,10˚S]. Between those plumes, the AOT retrieved above clouds by SEVIRI is relatively low at between 0.0 and 0.3. A very good spatial agreement is observed with the MOD06ACAERO product (fig. 2d), but the values are slightly larger than the SEVIRI AOT. For instance, the local average next to the coast is 0.8 for MODIS against 0.7 for SEVIRI. A strong visual agreement~~spatial correlation~~ is also observed between the cloud properties retrieved with SEVIRI (fig. 2b and 2c) and MODIS (fig. 2e and 2f). Both satellites detect shallow clouds with small droplets off the coast of Namibia and optically thicker clouds with larger droplets on the north-west part of the map. However, the CER retrieved by SEVIRI are smaller than the MODIS CER by~~- about~~ 2~~1.5~~ µm on average over the map. One can also see that the SEVIRI retrieval rejects more cloudy pixels than the MODIS one, especially in the more broken cloud regions in the south-west part of the region. For methods based on the colour ratio effect, the above-cloud AOT can only be retrieved when the cloud is bright enough. The SEVIRI algorithm rejects both the aerosol and cloud products when the COT is lower than 3 whereas the threshold of 4 on the COT of the MOD06ACAERO retrieval is used to reject the above-cloud AOT product only. This difference in the cloud sampling between the two methods can lead to a significant difference when comparing the regional mean of the above-cloud direct radiative effect (Zhang et al., 2016b). However, the 0.1° × 0.1° grid resolution used here is close to the typical resolution of global operational numerical weather predictions model that can examine the impact of clouds. Therefore, when comparing to global climate models (e.g. as per the model/POLDER comparison detailed in Haywood et al., 2020), users are advised to use a similar screening procedure to the satellite retrieval.

2.b.ii. Statistical comparisons

In this section, we extend our comparison of SEVIRI and MODIS retrievals of aerosol and cloud properties to 9 days of observations between the 28th August and 5th September 2017 (i.e. during the CLARIFY-2017 deployment of the BAe146 FAAM aircraft). During this time period, there were 34 MODIS overpasses between 0˚N - 30˚S and 20˚W - 15˚E. In addition to the filters described in section 2.a, observations associated with $CER_{SEVIRI} > 30$ µm are removed to be consistent with the upper limit of the MODIS retrieval. Figure 3 shows the correlation between the SEVIRI and MODIS retrievals of aerosol and cloud properties. The mean, median and standard deviation of the collocated data have been calculated for each satellite product and are summarized in Table 1.

Similar to the single case study reported in the previous section, a correlation (Pearson's correlation coefficient R of 0.78~~7~~) is evident between the SEVIRI and the MODIS above-cloud AOT. The error bars in Figure 3a represent the uncertainty associated with the retrieved AOT. In Peers et al. (2019), the uncertainty of the AOT retrieved by SEVIRI due to the aerosol, the cloud model, the Rayleigh scattering (i.e. the altitude of the aerosol and the cloud layer) and the water vapour correction have been estimated to be 40%, 0.3%, 2.5% and 10% respectively. The uncertainty due to the measurements has been estimated by calculating the standard deviation of the SEVIRI AOT in Figure 3a for each AOT bin. The total uncertainty is obtained by combining the uncertainties listed above, assuming they are independent (i.e. using the square root of the sum of squares). The MODIS uncertainty, which is provided by the algorithm, accounts for the above-cloud column two-way transmittance errors, the Rayleigh scattering errors, the measurement errors and the errors due to the aerosol and the cloud model. As with SEVIRI, the aerosol model assumption is typically the largest source of uncertainty in the MODIS retrieval (Meyer et al., 2015). Figure 3a shows that smaller values are retrieved by SEVIRI, with the straight-line fit of SEVIRI versus MODIS retrievals of AOT having a slope of 0.71. However, a non-linear relationship can be observed in Figure 3a between the two retrieved AOTs. A difference of 20.3~~6~~% is obtained in the mean values observed by the two satellites. This can be explained mainly by the differences in the aerosol model assumed for the retrieval. In the companion paper (Peers et al., 2019), it is shown that the assumed aerosol Single Scattering Albedo (SSA) can have a large impact on the retrieved above-cloud AOT. For the MOD06ACAERO algorithm, the assumed microphysical properties of aerosols are a function of the AOT (Levy et al., 2009). This results in an SSA at 0.55 µm of 0.86, 0.87 and 0.88 for an AOT of 0.1, 0.5 and 1.5, respectively. The aerosol model assumed for the SEVIRI retrieval is based on high quality aerosol size distribution data and high accuracy Cavity Ring Down (CRD) and Photo Ac~~e~~oustic Spectrometer (PAS) data (Davies et al., 2019; Taylor et al., 2020, Wu et al., 2020) measured by the FAAM aircraft in the vicinity of Ascension Island and has a fixed SSA of 0.85 (see section 3), which is more absorbing than the MODIS aerosol model. To reduce the influence of the assumed SSA on the results, the Absorbing AOT (AAOT) has been compared and is shown in Figure 3b. A better agreement is observed in the AAOT, with a slope of 0.87~~6~~ and a correlation coefficient of 0.78~~7~~. A slightly non-linear relationship is still observed between the two AAOTs with the SEVIRI AAOT smaller than the MODIS retrieval by 7.5~~9.4~~% on average. The SSA assumption not only has a large impact on the scattering AOT, it also influences, to a lesser extent, the AAOT. Peers et al (2019) also showed that the AAOT is sensitive to the assumed asymmetry factor. The asymmetry factor assumption for the MOD06ACAERO retrieval is AOT dependent (with the asymmetry factor taking values of 0.60 and 0.62 at a wavelength of 0.55 µm for AOT value of 0.5 and 1.5, respectively) and is smaller than the asymmetry factor assumed for the SEVIRI algorithm (i.e. 0.65 at 0.55 µm). To confirm that the aerosol model assumptions are the primary cause of differences in retrieved AOT, the SEVIRI retrieval has been run using both the CLARIFY-2017 and the MOD06ACAERO aerosol model for the case study described in section 2.b.i. The comparison of the both sets of AOT with MODIS is plotted in Figure 4. The slope of the regression line between SEVIRI and MODIS is 0.81 with the CLARIFY-2017 model and it is 1.05 when the same model (i.e. MOD06ACAERO model) is used. Moreover, the mean AOT for this case study is 0.44 for MODIS, 0.33 for SEVIRI using the CLARIFY-2017 model and 0.44 for SEVIRI using the MOD06ACAERO model. This confirms that, for AOT larger than 0.25, the differences between the SEVIRI and the MODIS retrieval are mainly due to the assumed aerosol properties. While the CLARIFY-2017 and ORACLES observations provide a thorough and comprehensive analysis of the BBA optical properties, which are adopted by the SEVIRI and MODIS satellite retrievals, representing the level of complexity of the variation of optical properties owing to evolution of flaming to smouldering combustion during the biomass burning season (Eck et al., 2003) and the complexity of aerosol aging processes (e.g. Wu et al, 2020; Taylor et al., 2020) is beyond current observational capabilities. The non-linearity of the AOT and AAOT comparison as well as the d~~D~~ifferences between the SEVIRI and MODIS distributions at low values can be partly explained by the MODIS filter on the AOT uncertainty. The signal to noise ratio being smaller at low AOT, ~~-~~the near zero AOT_{MODIS} ~~results being~~ are typically associated with an uncertainty larger than 100% and are discarded. Although no filters are applied to remove those results in the SEVIRI dataset, their contribution to the total DRE over the South-East Atlantic are expected to be small.

Figure 3c and 3d show the COT and CER comparisons and confirm the strong correlation (R=0.91) observed in the case study. The CER linear regression is characterised by a slope of 0.87 and an intercept of -0.8 µm, which indicates that the SEVIRI CER is generally smaller than the MODIS observations. On average, the CER values retrieved by SEVIRI and MODIS differ by 2.2 µm. For passive satellite sensors, the CER is typically retrieved from measurements in a water absorbing spectral band in the SWIR region. Here, the SEVIRI algorithm uses the 1.64 µm channel while the MODIS retrieval relies primarily on the 2.10 µm channel. Because of the different penetration depth of the reflected photons (Platnick, 2000), the MODIS retrieval of CER at 2.10 µm is sensitive to the upper cloud microphysics while the CER retrieved by SEVIRI at 1.64 µm is representative of the droplets lower down in the cloud. Therefore, as the droplet size increases from the base to the top of the cloud, the CER retrieved from the 2.10 µm channel should be larger than the CER retrieved from the 1.64 µm. To assess the impact of the difference of spectral band, the MOD06 CER retrieved from the 1.6 and 2.1µm channels from MODIS (Platnick et al., 2105) have been compared when the above-cloud AOT is lower than 0.5 for the case study presented earlier. The CER retrieved from the 1.6 µm channel is lower than the one retrieved from the 2.1µm by 0.5µm, which is consistent with the analysis from Platnick (2000). Differences in the cloud parametrisation, such as the refractive index and the effective variance, also affect the CER retrieval (Arduini et al., 2005; Painemal and Zuidema, 2011, Platnick et al., 2019), although the impact is expected to depend on the observed scattering angle. Biases could also arise from an offset in the absolute calibration of the SEVIRI 1.64 µm band compared to MODIS (Meirink et al., 2013).

A strong linear relationship is obtained between the SEVIRI and the MODIS COT and a difference of only 1.5 (10.5%) is observed between the two mean values, with the MODIS COT being larger on average. The agreement between the two satellites is better at lower COT and the differences increase with the COT. The spatial resolution of the instrument has an impact on the COT retrieval via the plane-parallel bias (Cahalan, 1994; Szczap et al., 2000, Zhang et al., 2006a). The relationship between the top-of-cloud reflectance and the COT is convex, which means that the COT derived from the mean reflectance of a pixel is smaller than the COT calculated from the mean COTs within the pixel. Zeng et al. (2012) have shown that subpixel inhomogeneities cause satellite sensors with a coarser spatial resolution, such as SEVIRI, to retrieve smaller COT. Also, as the clouds becomes thicker, the visible and the Near Infra-Red (NIR) measurements become less sensitive to the COT for both instruments. Using a radiative transfer code to simulate the SEVRI signal, we estimate that an error of +1.5 µm on the CER retrieved by SEVIRI causes a bias of +0.3 for a COT of 5.0 and +4.9 for a COT of 45. Therefore, differences in the retrieved CER could partly explain the low bias on the SEVIRI COT compared to MODIS at large COT.

Note that the cloud properties from SEVIRI and MODIS have also been compared for low above-cloud AOT (AOT < 0.05) to separate the impact of the aerosol correction from the cloud retrieval itself. The Figure S1 in the supplement shows that similar relationships are obtained with and without aerosol above clouds.

3. Comparison with CLARIFY-2017 measurements

3.a. Instruments

3.a.i. EXtinction, SCattering and Absorption of Light for AirBorne Aerosol Research (EXSCALABAR)

EXtinction, SCattering and Absorption of Light for AirBorne Aerosol Research (EXSCALABAR) is a state-of-the-art suite of spectrometers for measuring in situ aerosol optical properties aboard the UK research aircraft (FAAM BAe-146, https://www.faam.ac.uk). EXSCALABAR includes cavity ring-down spectroscopy (CRDS) and photoacoustic spectroscopy (PAS) instruments for the measurement of extinction and absorption coefficients at several wavelengths, respectively. We now describe briefly the measurement capabilities of EXSCALABAR and how it was operated during CLARIFY-2017, while the reader is referred to previous publications for complete details on calibration, operating principles and instrument descriptions (Davies et al., 2018; 2019; Cotterell et al., 2019a). In particular, Davies et al. (2019) outlined the same sample conditioning and operation of the spectrometers during the airborne measurements used in this work.

Four CRDS channels measured extinction at wavelengths of 405 and 658 nm, with three 405-nm channels measuring the extinction for aerosol at relative humidities (RH) of <10, 70 and 90% and the 658-nm channel operating under dry conditions (<10 % RH) only. The CRDS instruments use high finesse optical cavities formed from two highly reflective mirrors separated by ~40 cm to achieve total optical path lengths of order 5 – 11 km through the aerosol sample. Intensity modulated laser light is passively coupled into each optical cavity and a photodetector used to monitor the decay of light exiting the rear mirror following each on-off laser cycle. The signal exiting the cavity decays exponentially and is fitted to extract the 1/*e* folding time, referred to as the ring-down time. The change in ring-down time between an empty cavity (i.e. a sample devoid of any light scattering and absorbing aerosols) and a cavity filled with aerosol sample, enables the aerosol extinction coefficient α_{ext} to be calculated (Davies *et al.* 2018). The long path lengths achieved in CRDS provide measurements of aerosol extinction to a sensitivity better than 0.2 Mm^{-1} for 1-s sampling.

EXSCALABAR also included five PAS instruments that measured aerosol absorption coefficients under dry conditions (<10 % RH). Three PAS instruments sampled the dried aerosol directly, with each spectrometer operating at a different visible wavelength (405, 515 or 658 nm). Two further 405 and 658 nm spectrometers sampled aerosol that had additionally passed over a thermal denuder (a heated carbon catalyst) are used to remove semi-volatile organic aerosol components that can act to enhance light absorption by refractory components. However, the 658-nm spectrometer that sampled thermally denuded aerosol did not provide data during CLARIFY-2017 due to a faulty laser. Briefly, PAS measures light absorption coefficients for in situ aerosol in a non-contact manner (i.e. not using filter collection). Laser light is intensity-modulated to heat aerosol particles within an acoustic resonance cell, leading to the generation and amplification of a sound wave as particles liberate their heat to surrounding air. This sound wave is measured using a microphone and is directly proportional to the aerosol absorption coefficient, with the constant of proportionality determined by calibrating each PAS instrument using ozone-laden air with a known absorption coefficient. Again, we refer the reader to previous work on the principles of photoacoustic spectroscopy (Davies et al., 2018, Cotterell et al., 2019b), assess the accuracy of PAS aerosol absorption measurements (Davies et al., 2018), the calibration of PAS instruments with ozone (Cotterell et al, 2019a).

EXSCALABAR operated behind a 1μm diameter impactor to remove super-micron aerosols and sampled from the aircraft via a modified Rosemount inlet. It extracted an aerosol-laden sample from this inlet at a rate of 7 L min^{-1}. The sample underwent flow conditioning that included passing the sample through a Nafion dryer to dry the sample to <10 % RH and then through an NO_X/O_3 scrubber to remove gas phase species that would have otherwise contributed to the measured light extinction and absorption. The conditioned sample was split using a series of Brechtel precision flow splitters to provide samples to each spectrometer.

3.a.ii. Microwave Airborne Radiometer Scanning System (MARSS)

Previous studies (e.g., English 1995; Zuidema et al. 2012) have demonstrated that airborne millimeter-wave radiometers can be used to retrieve liquid water path (LWP) in stratocumulus clouds. Such microwave retrievals are not contaminated by the presence of absorbing biomass burning aerosol above clouds (e.g. Haywood et al., 2004). In this study, we use downward-looking views from the 89- and 157-GHz channels on the Microwave Airborne Radiometer Scanning System (MARSS) (McGrath and Hewison, 2001). Over the ocean, the downward-looking measurements are sensitive to absorption and emission by cloud liquid water as the sea surface provides a relatively cold radiative background due to its low emissivity at these frequencies. LWP retrievals using downward-looking MARSS observations on the FAAM aircraft have been used previously by Abel et al (2017) in their study of a cold-air outbreak. Our retrieval method is based on the Optimal Estimation Method (Rodgers, 1976) and is broadly similar to that described by English (1995). Radiative transfer simulations are performed using the Atmospheric Radiative Transfer Simulator (ARTS) model (Buehler et al. 2018), with background profiles of temperature and humidity taken from dropsondes released close to the location of the above-cloud runs. The surface emissivity is calculated using the fast ocean surface emissivity model FASTEM (Liu et al. 2010), with the surface temperature taken from infrared measurements during below-cloud runs and wind speed taken from the dropsondes. The cloud liquid water content is assumed to increase linearly from cloud base to cloud top, and the altitudes of the cloud base and top are estimated from aircraft profiles through the cloud layer. Cloud liquid water absorption is calculated using the Ellison (2007) model. The retrieved parameters are the liquid water path (LWP) and the column-integrated water vapour, which are used to scale the background profiles of liquid water content and water vapour in the forward model to provide the closest match to the observed brightness temperatures.

Errors in the MARSS LWP retrievals arise from several sources, including errors in the forward model used in the retrieval, the instrument noise and calibration errors. Instrument noise and calibration errors are estimated to be less than 1K, and the combined instrument and forward-model error in the retrieval is assumed to be uncorrelated with a standard deviation of 2K. The overall uncertainty in the retrieved LWP is estimated by combining the posterior error covariance from the retrieval with sensitivity estimates derived by perturbing fixed input parameters such as the sea surface temperature, wind speed, cloud top and base heights, and water vapour profile within plausible ranges. The total uncertainty is estimated to be approximately 40 g m^{-2} at low LWP (< 200 g m^{-2}) and it increases with increasing LWP becoming about 10-12% at large LWP (> 400 g m^{-2}).

3.a.iii. Cloud Droplet Probe (CDP)

The Droplet Measurement Technologies Cloud Droplet Probe (CDP) is a forward scattering optical particle counter which can detect particles over the nominal size range of 3 to 50 µm. Light from a 658 nm diode laser illuminates the sample volume and scattered light is collected over a 1.7 to 14° solid angle. The incoming beam is split using a 50:50 optical beam splitter, where one beam is focused through an optical mask before being sampled by a so-called *qualifier* photodetector and the other by the *sizer* detector. This detection configuration is used to qualify the depth of field (DOF) where the signal from the qualifier detector multiplied by two must exceed the signal from the sizer for the particle to register as being measured within the DOF. Particles which do not meet this criterion are rejected. The signal pulses from DOF accepted particles are digitised from their raw analogue voltages; the peak value corresponding to the scattering cross section is then segregated into one of 30 bins and the sum of counts in each bin over the sampling integration period is transmitted to a logging computer running PADS (version 3.11) software.

A 10-point glass bead calibration spanning the instrument's detection range was performed before each day of flying throughout the CLARIFY-2017 campaign. The nominal bead size is corrected for the differences between the refractive indices of glass and water and the water corrected size is used to calibrate the instrument's sizing response. The calibration was found to be consistent across the campaign, resulting in an approximate 7% under-sizing correction being applied to the instrument's sizing response.

3.b. Atmospheric profile

The atmospheric correction is an essential step of the SEVIRI aerosol-above-cloud retrieval. The spectral contrast between the 0.6 and the 0.8 µm channels, which is used to retrieve the above-cloud AOT, is especially sensitive to the absorption from water vapour (Peers et al., 2019). To remove the contribution of water vapour from the signal, the transmittances from the cloud top to the top of the atmosphere are calculated using the humidity profiles from the operational forecast configuration of the global Met Office Unified Model (Brown et al., 2012) and the cloud top height retrieved from the SEVIRI infrared channels (Francis et al., 2008, Hamann et al., 2014). The humidity and temperature profiles used in the correction scheme are evaluated against those from the dropsondes deployed during the CLARIFY-2017 flights. Figure 5 shows the location of the flights analysed in this paper. Note that owing to difficulties in transmitting data from such a remote location, the dropsonde measurements from the campaign have not been assimilated in the model forecasts. The above-cloud and the full column integrated water vapour are calculated from the sondes and the forecast profiles. For both the model and the measurements, the highest altitude is considered to be the altitude at which the sonde has been dropped and, for the full-column integration, the bottom altitude corresponds to the lowest altitude measured by the sonde. To be consistent with the atmospheric correction scheme, the above-cloud water vapour from the forecast is calculated using the cloud top height from SEVIRI. For the dropsondes, the cloud top height is defined at the altitude of the temperature inversion, which is consistent with lidar and in situ observations from the aircraft (e.g. Haywood et al., 2020). To assess the added value brought by the forecast model, the water vapour content has been calculated for the tropical atmospheric profile from McClatchey et al. (1972) using the cloud top height retrieved with SEVIRI. Figure 6 shows the integrated water vapour comparison of the dropsondes, the forecast and the McClatchey atmospheric model. The dew point and temperature profiles from the dropsonde, the NWP model and the McClatchey model are shown for each flight in Figure S2 of the supplement. The NWP and the McClatchey integrated column water vapour above cloud are plotted against the measurements from the dropsonde in Figure S3 of the supplement. The problem in assuming a single profile for water vapour from McClatchey climatologies is evident from the gross overestimation of water vapour and the limited variability which comes only from changes in the cloud height (R=0 in fig. S3). When NWP model data is used, the amount of water vapour used for the atmospheric correction is strongly correlated with the dropsonde observations (R=0.89 in fig. S3) but the integrated water vapour path is larger by 3.1 mm on average compared to the dropsonde measurements. On the other hand, the full column water vapour from the forecast and the observations follow the same trend with a mean absolute difference of 1.5 mm in integrated water vapour path. Much of this difference is explained by the underestimation of the altitude of the cloud top retrieved by SEVIRI, with a mean bias of -265 m. When the cloud top height from the dropsonde is used to calculate the integrated water vapour above cloud from the forecast, the absolute difference to the measurements is reduced to 0.7 mm on average, which indicates a reasonable performance of the model in forecasting the vertical profile of humidity. The SEVIRI cloud top height retrieval is derived by conversion of the observed brightness temperature to a cloud top height assuming the temperature profile from the Met Office forecasts. Therefore, a reasonable consistency is observed between the retrieved cloud top height and the altitude of the temperature inversion from the model, with an absolute difference of 88 m. The individual profiles shown in Figure S2 in the supplement show that the model does not quite capture the depth of the boundary layer. However, no evidence of a correlation between the cloud top height error and the presence of absorbing aerosols in the boundary layer has been observed. While identifying the causes of these biases is complex and beyond the scope of this paper, it is worth mentioning that the boundary layer depth in the model is highly influenced by the balance between the subsidence and the entrainment rate.

The overestimation of the water vapour in the atmospheric correction, which disproportionately affects the 0.8µm channel where water vapour absorption is stronger (see Figure 3 in Peers et al., 2019), indicates that an overestimation of the above-cloud AOT retrieved by SEVIRI may be expected due to an artificially enhanced spectral contrast between 0.6 and 0.8µm. In Figure 5, one can see that the dropsondes have been launched in a small region around Ascension Island. Its remote location implies that the number of highly accurate measurements available for model assimilations is limited to the radiosonde releases from Ascension Island and therefore relies heavily on vertically-integrated atmospheric state variables retrieved from satellites. Therefore, it might reasonably be expected that the performance of the forecast model and the cloud top height retrieval could vary with the distance from the African continent where radiosonde launches are less sparse. In the absence of in situ atmospheric sounding between Ascension Island and the African coast, the comparison of the above-cloud aerosol properties retrieved from SEVIRI and MODIS can be considered as an indirect evaluation of the atmospheric correction scheme, since the MODIS channels used for the retrieval are barely impacted by the absorption from water vapour, provided that the differences due to the assumptions on the aerosol microphysical properties are accounted for. To minimize the influence of the aerosol model differences between the two retrievals, we have chosen to compare the AAOT. The SEVIRI and the MODIS collocated observations from section 2.b.ii (i.e. from 28th August to 5th September 2017 and over 0˚N - 30˚S and 20˚W - 15˚E) have been used, removing $AAOT_{SEVIRI}$ lower than 0.03. Figure 7 shows the difference Δ of the mean AAOT as a function of the longitude, with ΔAAOT defined as:

$$\Delta AAOT = (AAOT_{SEVIRI} - AAOT_{MODIS}) / AAOT_{MODIS} \times 100\% \quad (1)$$

An increase of ΔAAOT can be observed from east to west. The $AAOT_{SEVIRI}$ is 8.3% smaller than the $AAOT_{MODIS}$ close to the continent. The sign of the difference changes at 2.7˚E. From the west of 5˚W, a sharp increase of ΔAAOT is observed, reaching 28.8% at 15˚W. This trend between SEVIRI and MODIS may therefore be related to a trend in the accuracy of the atmospheric correction scheme. As explained in section 2.b.ii, the AAOT from SEVIRI is expected to be slightly smaller than MODIS because of the different assumptions on the SSA and the asymmetry factor. The small low bias on the SEVIRI AAOT compared to MODIS suggests a good performance of the forecast model and the cloud top height retrieval next to the coast. From the coast to 9˚W, the difference between the SEVIRI and the MODIS AAOT is lower than 10%. In Figure 7, the longitudes associated with the dropsonde measurements are indicated by the grey lines and corresponds to the region where ΔAAOT is the largest. Therefore, the overestimation of humidity in the forecast model (as demonstrated in Figure 6) is likely a major contributor to biases in SEVIRI retrievals of AAOT, particularly at remote locations where very little observation data for humidity is available for assimilation into model forecasts. While our analysis suggests that errors in humidity in the model may well be the cause of the zonal discrepancy between the AAOT in MODIS and SEVIRI, we cannot definitively conclude this is the case. More detailed comparisons of atmospheric moisture fields from other high quality observations such as from the ORACLES or AEROCLO-sA vertical profiles against those from the Unified model would be necessary, but this is beyond the scope of the present work.

3.c. Aerosol layer

To survey the full column of aerosols and characterise the aerosol-radiation interactions, a series of manoeuvres described as a Z-pattern were performed on multiple flights during the campaign (Haywood et al., 2020). These patterns start at an altitude of about 7 km with a straight level run and dropsonde deployment above the aerosol plume, followed by a 180˚ turn and a profile descent through the main aerosol layers to an altitude of around a couple hundred meters above the cloud top. Then, a level 180˚ turn and another straight level run was performed along the same ground position as the upper run. Finally, subsequent to a further reciprocal turn, a profile descent was made through the cloud to 50 ft above sea-level. The extinction and absorption measured from EXSCALABAR during the two-part descent profiles have been used to calculate the total and absorption AOT above clouds at the wavelengths of the instrument and interpolated to 0.55 µm. The above-cloud AOT from SEVIRI has been obtained by averaging the observations acquired during the descent (i.e. four to five 15-minute time-slots) over an area within a 60-km radius from the position of the aircraft in the middle of the profile descent, which covers roughly the distance travelled by the aircraft. Additionally, the above-cloud AOT retrieved from the closest MODIS overpass (i.e. Terra in the morning and Aqua in the afternoon) have been averaged over the same area as SEVIRI. The impact of the time difference between the MODIS and the aircraft observations (lower than 2h30) on the AOT comparison is assumed to be negligible as the time and space variation of the aerosol distribution is expected to be small over this timescale.

The comparison of the above-cloud AOT from the in situ and the satellite measurements is presented in Figure 8. The darker colours represent the AAOT contribution to the AOT and the error bars correspond to the standard deviation calculated for each flight of the MODIS and SEVIRI AOT retrieved within the 60 km radius. The (nominally dry aerosol) SSAs obtained at 0.55 µm from EXSCALABAR for each flight are indicated above the in situ measurement bars. Note however, that in the free troposphere above the marine boundary layer, the relative humidity is typically around 30% and hence any hygroscopic growth is likely to be small (i.e. lower than 2% according to Magi and Hobbs, 2003). For clarity, the AAOT bar chart comparison is also shown in Figure S4 in the supplement. Given the limited size of the dataset, the consistency observed between the SEVIRI above-cloud AOT and the in situ measurements, which is shown in Figure S5 of the supplement, is promising (R=0.75). Except for flights C044 and C051, the above-cloud AOT measured by EXSCALABAR is within the standard deviation of the mean AOT retrieved from both SEVIRI and MODIS. The SSA derived from EXSCALABAR ranges from 0.798 to 0.858, suggesting some variations in the level of aerosol absorption. The SSA assumed for both satellite retrievals (i.e. SSA_{MODIS}≈0.87 and SSA_{SEVIRI}≈0.85) are in the upper bound of this range. As shown in Peers et al. (2019), colour-ratio based retrieval method are sensitive to the aerosol absorption above clouds which means that the retrieval of the AAOT above cloud is less sensitive to the assumed SSA than the AOT. This could explain why a better agreement is obtained between the in situ measurements and the satellite products on the AAOT than on the AOT for all flights except C044, C048 and C051. Both satellite AOTs for flight C044 are larger than $AOT_{EXSCALABAR}$, but the AAOT from EXSCALABAR and MODIS are in agreement while the AAOT from SEVIRI is larger. Contrary to SEVIRI, the MODIS channels used for the retrieval are barely impacted by the absorption from above-cloud water vapour. The AOT differences observed for this flight are consistent with the large overestimation of the water vapour by the SEVIRI atmospheric correction scheme in this case, as observed in Figure 6. For C048, the AOT retrieved from MODIS and SEVIRI are associated with especially large standard deviations. Although the in situ AOT is within the spread of the satellite retrievals, AOT_{SEVIRI} is about 47% larger than EXSCALABAR while AOT_{MODIS} is about 32% smaller. As confirmed by the satellite images, broken cloud cover was observed during this flight. Additionally, the SEVIRI and MODIS observations indicate that the in situ measurements were performed at the south-western edge of an aerosol plume where strong aerosol gradients were present. The low cloud fraction together with the strong above-cloud AOT gradient in this region could explain the differences observed between the satellite retrievals and the in situ measurements. Finally, both satellite retrievals overestimate the above-cloud AOT measured by the aircraft during C051. The overestimation from SEVIRI cannot be totally attributed to the atmospheric correction scheme because the AOT from SEVIRI is consistent with MODIS.

Information on the vertical profile of aerosols can be used to further investigate the differences between satellite observations and in situ measurements. After the descent profile through the aerosol layer, a profile descent through the cloud was typically performed which allowed sampling of marine boundary layer aerosols directly underneath the clouds. Table 2 summarises the extinction measured by EXSCALABAR directly above and under the stratocumulus cloud layer as well as the collocated CER retrieved by SEVIRI and MODIS. Note that the MODIS observations do not temporally correspond to the SEVIRI and EXSCALABAR measurements and that the purpose here is to illustrate the differences in the cloud properties between the flights. The collocated CER averaged over the CDP transect for flights C042 to C050 is around 9.1 µm for SEVIRI and 11.3 µm for MODIS. For C051, both satellites retrieve significantly smaller droplets, with a difference of 2.8 µm and 3.4 µm for SEVIRI and MODIS respectively, which could potentially be caused by aerosol-cloud interactions. In addition, in situ measurements indicate that the air directly underneath the stratocumulus cloud is 3.2 times more polluted for flight C051 than for the other flights, suggesting a significant entrainment of BBA into the MBL. Figure 9a and 9b show the CER retrieved by SEVIRI and MODIS as a function of the extinction measured respectively directly above and below the cloud. While the correlation obtained with the above-cloud extinction is moderate (R=0.58), there is a convincing relationship between below-cloud extinction and the CER (R=0.86). Although these results are far from robust considering the limited number of measurements available, this is consistent with the observations from Diamond et al. (2018). Using data from the ORACLES campaign, they observed a correlation between the presence of smoke in the marine boundary layer and changes in the cloud microphysics. They have also reported that the presence of smoke directly above cloud is not necessarily an indicator of aerosol-cloud interactions because of the mixing of elevated smoke into the boundary layer typically takes a couple of days. Pollution within clouds tends to increase the cloud albedo of by acting as cloud condensation nuclei but can also increase their absorption coefficient (Twomey, 1977). Although the brightening of the clouds is typically the dominant effect, the presence of absorbing smoke within the cloud could have an impact on the spectral variation of the cloud reflectance. Both the SEVIRI and the MODIS algorithms assume that the entire aerosol layer is located above an unpolluted cloud and do not account for aerosols within the cloud. Therefore, a reduction in the cloud albedo in the visible/SWIR range due to pollution within the cloud layer could be interpreted by colour-ratio based retrievals as an additional aerosol signal, leading to an overestimation of the above-cloud AOT.

3.d. Cloud layer

3.d.i. Cloud droplet Effective Radius (CER)

The cloud droplet size distribution has been measured with a CDP during straight level runs at about 100 m below the cloud top. Figure 10 shows the time-series of the CER measured by the aircraft (blue dot) with the closest SEVIRI retrieval in space and time (red line). In addition to the aerosol-above-cloud algorithm, the CER has been retrieved considering an above-cloud AOT of zero and is plotted in orange. The grey areas represent the pixels that have been rejected by the algorithm's filters, which include measurements poorly fitted by the algorithm, observations in the backscattering glory region, COT lower than 3, cloud edges and inhomogeneous clouds (section 2a). The CER retrieved from SEVIRI is plotted against the CDP measurements in Figure S6 of the supplement. The consistency observed between the in situ measurements and the satellite retrievals is good (R=0.77 in fig. S6) with both the variation in CER during a single flight and the inter-flight differences being well represented. The range and the variation of the CER is well reproduced by SEVIRI, especially for the flights C044, C049 and C051 for which the mean difference between the satellite and the CDP is less than 0.4 µm. On the other hand, the valid CER retrieved by SEVIRI is on average 1.5 µm lower than the aircraft measurements over the C050 transect. Compared to the other flights, there is a stronger variability in the CER measured during C050. One-dimensional cloud properties retrievals, such as the SEVIRI aerosol-above-cloud algorithm, tend to underestimate the CER in case of subpixel heterogeneity (Marshak et al., 2006; Zhang and Platnick, 2011; Zhang et al., 2012; 2016a). Time differences between the aircraft and the satellite observations also add uncertainty in the comparison of the cloud properties, especially when the cloud layer changes quickly. In Figure 10c, a mirror-image symmetry in the CDP measurements is observed before and after 16:09. This is caused by a 180-degree turn performed by the aircraft between 16:08 and 16:10 followed by a slightly offset reciprocal run to fly through the same cloud. The fact that the CER measured at the end of this run (i.e. after 16:18) are smaller by about 2 µm than the CER measured at the beginning of the first run (between 15:55 and 15:58) suggests a relatively fast evolution of the cloud and/or an inadequate horizontal or vertical offset in the reciprocal leg. The vertical distribution of the CER has also an influence on the comparison with the satellite retrieval as the altitude of the measurements could differ from the expected peak of the vertical weighting function of the SEVIRI 1.64µm channel. Although the aircraft was flying at a constant altitude during the CDP measurements, it is difficult to precisely assess the relative position of the cloud top. Finally, we note that the impact of not taking the biomass burning aerosol layer above the cloud into account usually leads to an underestimation of less than 1 µm on the CER. In the grey areas of fig. 10b and 10c, unrealistically large cloud droplets are retrieved by the aerosol-above-cloud algorithm at the beginning of the C049 transect and just before and after the turn at 16:09 during C050. As confirmed by the aircraft observations, these pixels correspond to cloud edges. For partially cloudy fields of view, the darker portions of the pixel (either clear sky or optically thinner cloud) decrease the reflectance resulting in an increase of the retrieved CER (Zhang et al., 2012). These biases confirm that the filters implemented for the aerosol-above-cloud retrieval are useful in enhancing the quality of the SEVIRI retrieval products.

3.d.ii. Liquid Water Path (LWP)

The LWP has been retrieved using the microwave measurements from the MARSS instrument during the lower altitude straight level runs of the Z-patterns. ~~It is compared with the LWP derived from the COT and the CER retrieved by SEVIRI using the following relationship~~The dominant cloud regime around Ascension Island typically consists of a stratocumulus layer above shallow cumulus (Zhang and Zuidema, 2019). For the flights selected here, the CDP measurements from the vertical profiles indicate that the shallow cumulus layer consisted of smaller droplets than the upper stratocumulus and that the liquid water content increases with height. Considering an adiabatic cloud, the LWP from SEVIRI is derived from the retrieved COT and CER using the following relationship: ~~(Stephens, 1978)~~:

$$LWP_{SEVIRI} = \frac{\cancel{2}5}{\cancel{3}9}\rho_l \times COT \times CER \quad (2)$$

where ρ_l is the density of liquid water. It should be noted that the effective radius at the cloud top is expected to be slightly larger than the CER retrieved by SEVRI because of penetration depth effects (Platnick, 2000), which could lead to a small underestimation of the LWP from SEVIRI. It is also important to add that the MARSS retrieval makes no distinction between cloud liquid and precipitation, and returns the total liquid water path. On the other hand, the LWP obtained from SEVIRI does not account for precipitation. Therefore, the LWP from MARSS is expected to be larger than SEVIRI in the presence of rain and drizzle drops.

Although the aircraft measurements are collocated with the closest SEVIRI retrieval in space and time, the cloud field is expected to change between consecutive SEVIRI observations. To optimise the analysis against the satellite retrieval, we have selected the flights for which the cloud field changed the least between the observations from the top and the bottom leg of the Z-pattern by visual inspection of the radiometer signal.

Figure 11a, 11b and 11c shows the LWP from MARSS (blue) and from the SEVIRI aerosol-above-cloud algorithm (red) against the time (UTC) of the aircraft measurements for the flights C042, C049 and C050 respectively. Additionally, the LWP from SEVIRI is plotted against the MARSS retrieval in Figure S7 in the supplement. Although a moderate correlation is obtained (R=0.56 in fig. S7), similarities can be observed between the variations of LWP_{MARSS} and LWP_{SEVIRI}. The observations during the C042 transect contain two main features: the first one is detected by MARSS and SEVIRI between 10:06 and 10:11 while the second one (between 10:12 and 10:17) appears slightly earlier in the satellite retrieval. The collocated LWP_{SEVIRI} also seems to be shifted to an earlier time by about 1 minute compared to MARSS for C049 and C050. Differences are also observed, notably during C050 (fig. 11c) between 15:27 and 15:30 where LWP_{MARSS} ranges from 100 to 170g m^{-2} and LWP_{SEVIRI} is around 45 ~~50~~g m^{-2}. Such discrepancies and shifts can be introduced by the differences in sampling time between the aircraft and the SEVIRI snapshot. We also note the large range of values obtained by MARSS, with LWP up to 868 g m^{-2}. Such a high LWP translates into a COT of 156~~130~~ for a CER of 10 µm. On the other hand, the maximum LWP reached by the satellite retrieval is much lower, with a value of 514~~616~~ g m^{-2}. ~~The main cause is~~It should be noted that the COT upper bound in the look up tables used for the SEVIRI algorithm~~ which~~ has been set to 80 for computational efficiency. However, the proportion of clouds with COT larger than 80 is expected to be negligible on the regional scale as 99% of the SEVIRI observations used in fig. 3b have a COT lower than 40. An underestimation of the COT ~~caused by~~ due to the plane parallel bias (Cahalan et al., 1994; Szczap et al., 2000) can also cause lower LWP in the satellite observations. Moreover, the peaks of LWP from MARSS and the overall larger values than SEVIRI could also be attributed to the contribution of drizzle and precipitation which is not accounted for in the LWP derived from the satellite. In-flight visual observations report drizzle during the 3 flights and droplets with an effective radius larger than 100 µm were detected by a 2 Dimensional Stereo probe during C049 and C050. There is no clear evidence of precipitation in the measurements from the vertical profiles but it is difficult to completely discount this type of local precipitation events during the long runs above cloud top that were performed with MARSS. Considering the time mismatch issues and the technical limits of the algorithm, there is a very satisfactory agreement between the LWP retrieved from the aerosol-above-cloud retrieval and the aircraft observations.

The LWP retrieved by SEVIRI when the above-cloud AOT is forced to 0 is shown in Figure 11 in orange. As expected, omitting the presence of absorbing aerosol leads to an underestimation of the LWP from passive remote sensing instrument (e.g. Haywood et al., 2004), with a mean bias of 55.8~~64~~ g m^{-2}. Table 3 compares the mean LWP from MARSS and SEVIRI for each flight as well as the mean COT and CER retrieved from satellite with and without taking into account the aerosol absorption above the clouds. The impact of the biomass burning aerosol on the CER retrieval is lower than 0.8 µm and therefore represents only a small fraction of the bias on the LWP. However, the "no aerosol" retrieval underestimates the COT by 34.7% compared to the aerosol-above-cloud algorithm, which account for 93.2% of the bias on the retrieved LWP.

4. Discussion and Conclusions

The objective of this paper is to assess the performance of the SEVIRI retrieval of aerosol and cloud properties in cases where aerosols overlie clouds. The first part of the exercise consisted of the intercomparison of the MODIS and the SEVIRI products. Although both algorithms rely on the colour-ratio effect, the analysis shows the impact of the satellite instrument characteristics and the choice of the aerosol model assumption on the retrieved aerosol and cloud properties. The above-cloud AOT from SEVIRI is found to be lower than MODIS by 20.3~~16.5~~%. This is mainly attributed to the fact that the aerosol model assumed for the SEVIRI retrieval is more absorbing than MODIS. Regarding the cloud properties, a very good agreement is observed on the COT while the CER from SEVIRI is consistently smaller than MODIS by 2.2 ~~~2~~µm. The latter is partly explained by the difference of spectral band used for the retrieval (i.e. 1.64 µm for SEVIRI and 2.1 µm for MODIS) which implies different penetration depths of the photons inside the clouds.

Secondly, the SEVIRI products have been validated against a set of in situ and remote sensing measurements from a research aircraft platform during the CLARIFY-2017 field campaign. Water vapour profiles from dropsondes were used to evaluate the atmospheric correction scheme. The analysis has revealed that the algorithm tends to overestimate the amount of water vapour above clouds around the CLARIFY-2017 region, which should lead to an overestimation of the AOT. The comparison of the measured profiles with the forecast revealed that the overestimation of the water vapour above cloud is caused by an underestimation of the cloud top height retrieved by SEVIRI by an altitude of 260 m on average. Comparison of the absorbing AOT from SEVIRI and MODIS suggests that the accuracy of the atmospheric correction scheme is likely to be better closer to the coast, where the largest amounts of biomass burning aerosols are observed.

The AOT was calculated above clouds based on the extinction profiles from EXSCALABAR for eight flights. The satellite retrieval is found to overestimate the AOT when the sampled aerosols are more absorbing than the assumed aerosol model but a better agreement is obtained on the above-cloud AAOT. We also observed an overestimation of the AOT in a case where measurements suggest interaction between aerosol and cloud droplets. The CER from SEVIRI has been validated against the cloud droplet size measured by the aircraft-mounted CDP. The LWP has been calculated from the COT and CER retrieved from SEVIRI and compared to the microwave measurements from MARSS. The main cause of discrepancies in the cloud properties appears to be the temporal mismatch between SEVIRI and the aircraft measurements.

Although the variations of the satellite LWP follows those of the aircraft observations, the LWP obtained from SEVIRI is typically smaller than the measurements from MARSS. The drizzle observed during these flights partly explain this discrepancy as the LWP from SEVIRI does not account for drizzle and rain while the MARSS instrument does. An underestimation of the LWP due to an underestimation of the COT by SEVIRI can also be expectedhas been observed in case of extremely large LWP (i.e. > 7600 g.m^{-2}) because the algorithm is limited to a COT of 80. Given the limitations inherent to this validation exercise and the technical restrictions of the retrieval, a good agreement has been observed between the satellite products and the aircraft measurements. As expected, biases are observed on the cloud properties retrieved without considering the aerosol absorption above-cloud, notably on the COT which accounts for 93% of the low bias obtained on the LWP.

Validation and intercomparison exercises are necessary to provide confidence in the satellite-based retrievals and to understand their limitations. In the present paper, we have identified two main sources of uncertainty on the SEVIRI aerosol-above-cloud products: the accuracy of the atmospheric correction and the assumed microphysical model of aerosol, especially the SSA. For the former, the overall agreement between MODIS and SEVIRI shows that the atmospheric correction method relying on model forecast humidities appears satisfactory. Although its accuracy decreases far from the coast, the use of the water vapour profiles from the forecast is a significant improvement compared to the use of simple standard atmosphere climatological values.

Regarding the assumed microphysical properties of the aerosol, the recent field campaigns (Zuidema et al., 2018; Pistone et al., 2019; Taylor et al., 2020; Wu et al., 2020) have examined the variability of the SSA of biomass burning aerosol over the SEAO. Although the aerosol model used for the retrieval is based on in situ observations from CLARIFY-2017, using a single aerosol model to retrieve the above-cloud AOT is a limitation. However, accounting for the variability of the aerosol microphysical properties in current satellite retrievals is not currently possible. Given the algorithmic assumptions and the technical limitations, the consistency observed between SEVIRI, MODIS and the airborne measurements is encouraging, which indicates that the geostationary instrument is able to provide complementary information on aerosols above clouds. These high temporal resolution observations would significantly enhance our knowledge on the aerosol interaction with both radiation and cloud as well as the aerosol transport in a region associated with the largest inter-model differences. The longitudinal variations in AAOT caused by inaccuracies in the atmospheric correction are unlikely to cause significant problems in assessing the temporal evolution of BBA plume radiative forcing over short timescales, but need to be borne in mind when assessing longer range plume transport.

The validation of a satellite retrieval needs a large number of observations and the analysis presented here can be considered as a first step in an ongoing continuous effort. Other datasets, such as the measurements from ORACLES and AEROCLO-sA field campaigns, can help to further assess the accuracy of the algorithm and will be the subject of future work.

Data availability

The SEVIRI data used for this study are available from the corresponding author, FP, upon reasonable request. MODIS above-cloud data products are available from KGM upon request. The FAAM aircraft data are archived at the Centre for Environmental Data Analysis (CEDA).

Author contributions

FP, PF and JMH developed the concept and the ideas for this paper. PF implemented the atmospheric correction scheme and FP the SEVIRI retrieval algorithm. The SEVIRI products have been processed by FP. KGM and SEP developed the MOD06ACAERO retrieval and generated the MODIS data. CF, SJA, KS, MIC, NWD and JML operated, calibrated and prepared the in situ measurements from EXSCALABAR. KNB and IC operated, calibrated and prepared the CDP measurements. SF calibrated the MARSS measurements and retrieved the LWP. FP carried out the analysis and prepared the paper with contributions from all co-authors.

Acknowledgements

We thank the Natural Environment Research Council (NERC) and the Norwegian Research Council for their financial support. Airborne data were obtained using the BAe-146 Atmospheric Research Aircraft operated by Directflight Ltd. and managed by Facility for Airborne Atmospheric Measurements (FAAM), which is jointly supported by NERC and the Met Office.

Financial support

This research has been supported by the Natural Environment Research Council (NERC) via the CLARIFY-2017 project (grant no. NE/L013479/1) and the Research Council of Norway via the projects AC/BC (grant no. 240372) and NetBC (grant no. 244141).

References

Abel, S. J., Boutle, I. A., Waite, K., Fox, S., Brown, P. R., Cotton, R., Lloyd, G., Choularton, T. W., and Bower, K. N.: The role of precipitation in controlling the transition from stratocumulus to cumulus clouds in a Northern Hemisphere cold-air outbreak, Journal of the Atmospheric Sciences, 74, 2293–2314, https://doi.org/10.1175/JAS-D-16-0362.1, 2017.

Abel, S. J., Barrett, P. A., Zuidema, P., Zhang, J., Christensen, M., Peers, F., Taylor, J. W., Crawford, I., Bower, K. N., and Flynn, M.: Open cells exhibit weaker entrainment of free-tropospheric biomass burning aerosol into the south-east Atlantic boundary layer, Atmos. Chem. Phys., 20, 4059–4084, https://doi.org/10.5194/acp-20-4059-2020, 2020.

Arduini, R., Minnis, P., Smith Jr, W., Ayers, J., Khaiyer, M., and Heck, P.: Sensitivity of satellite-retrieved cloud properties to the effective variance of cloud droplet size distribution, Tech. rep., Science Applications International Corporation, Hampton, Virginia; NASA, https://www.osti.gov/servlets/purl/84157, 2005.

Brown, A., Milton, S., Cullen, M., Golding, B., Mitchell, J., and Shelly, A.: Unified modeling and prediction of weather and climate: A 25-year journey, Bulletin of the American Meteorological Society, 93, 1865–1877, https://doi.org/10.1175/BAMS-D-12-00018.1, 2012.

Buehler, S. A., Mendrok, J., Eriksson, P., Perrin, A., Larsson, R., and Lemke, O.: ARTS, the Atmospheric Radiative Transfer Simulator version 2.2, Geoscientific Model Development, 11, 1537–1556, https://doi.org/10.5194/gmd-11-1537-2018, 2018.

Cahalan, R. F., Ridgway, W., Wiscombe, W. J., Bell, T. L., and Snider, J. B.: The Albedo of Fractal Stratocumulus Clouds, Journal of the Atmospheric Sciences, 51, 2434–2455, https://doi.org/10.1175/1520-0469(1994)051<2434:TAOFSC>2.0.CO;2, 1994.

Chand, D., Anderson, T., Wood, R., Charlson, R., Hu, Y., Liu, Z., and Vaughan, M.: Quantifying above-cloud aerosol using spaceborne lidar for improved understanding of cloudy-sky direct climate forcing, Journal of Geophysical Research: Atmospheres, 113, https://doi.org/10.1029/2007JD009433, 2008.

Chang, I. and Christopher, S. A.: Identifying Absorbing Aerosols Above Clouds From the Spinning Enhanced Visible and Infrared Imager Coupled With NASA A-Train Multiple Sensors, IEEE Transactions on Geoscience and Remote Sensing, 54, 3163–3173, https://doi.org/10.1109/TGRS.2015.2513015, 2016.

Cotterell, M. I., Orr-Ewing, A. J., Szpek, K., Haywood, J. M., and Langridge, J. M.: The impact of bath gas composition on the calibration of photoacoustic spectrometers with ozone at discrete visible wavelengths spanning the Chappuis band, Atmospheric Measurement Techniques, 12, 2371–2385, https://doi.org/10.5194/amt-12-2371-2019, 2019a.

Cotterell, M. I., Ward, G. P., Hibbins, A. P., Haywood, J. M., Wilson, A., and Langridge, J. M.: Optimizing the performance of aerosol photoacoustic cells using a finite element model. Part 1: Method validation and application to single-resonator multipass cells, Aerosol Science and Technology, 53, 1107–1127, https://doi.org/10.1080/02786826.2019.1650161, 2019b.

Davies, N. W., Cotterell, M. I., Fox, C., Szpek, K., Haywood, J. M., and Langridge, J. M.: On the accuracy of aerosol photoacoustic spectrometer calibrations using absorption by ozone, Atmospheric Measurement Techniques, 11, 2313–2324, https://doi.org/10.5194/amt- 11-2313-2018, https://www.atmos-meas-tech.net/11/2313/2018/, 2018.

Davies, N. W., Fox, C., Szpek, K., Cotterell, M. I., Taylor, J. W., Allan, J. D., Williams, P. I., Trembath, J., Haywood, J. M., and Langridge, J. M.: Evaluating biases in filter-based aerosol absorption measurements using photoacoustic spectroscopy, Atmospheric Measurement Techniques, 12, 3417–3434, https://doi.org/10.5194/amt-12-3417-2019, https://www.atmos-meas-tech.net/12/3417/2019/, 2019.

de Graaf, M., Tilstra, L. G., Wang, P., and Stammes, P.: Retrieval of the aerosol direct radiative effect over clouds from spaceborne spectrometry, Journal of Geophysical Research: Atmospheres, 117, https://doi.org/10.1029/2011JD017160, https://agupubs.onlinelibrary.wiley.com/doi/abs/10.1029/2011JD017160, 2012.

de Graaf, M., Schulte, R., Peers, F., Waquet, F., Tilstra, L. G., and Stammes, P.: Comparison of south-east Atlantic aerosol direct radiative effect over clouds from SCIAMACHY, POLDER and OMI–MODIS, Atmos. Chem. Phys., 20, 6707–6723, https://doi.org/10.5194/acp-20-6707-2020, 2020.

Deaconu, L. T., Waquet, F., Josset, D., Ferlay, N., Peers, F., Thieuleux, F., Ducos, F., Pascal, N., Tanré, D., Pelon, J., and Goloub, P.: Consistency of aerosols above clouds characterization from A-Train active and passive measurements, Atmospheric Measurement Techniques, 10, 3499–3523, https://doi.org/10.5194/amt-10-3499-2017, https://www.atmos-meas-tech.net/10/3499/2017/, 2017.

Diamond, M. S., Dobracki, A., Freitag, S., Small Griswold, J. D., Heikkila, A., Howell, S. G., Kacarab, M. E., Podolske, J. R., Saide, P. E., and Wood, R.: Time-dependent entrainment of smoke presents an observational challenge for assessing aerosol–cloud interactions over the southeast Atlantic Ocean, Atmospheric Chemistry and Physics, 18, 14623–14636, https://doi.org/10.5194/acp-18-14623-2018, https://www.atmos-chem-phys.net/18/14623/2018/, 2018.

Eck, T. F., Holben, B. N., Ward, D. E., Mukelabai, M. M., Dubovik, O., Smirnov, A., Schafer, J. S., Hsu, N. C., Piketh, S. J., Queface, A., Roux, J. L., Swap, R. J., and Slutsker, I.: Variability of biomass burning aerosol optical characteristics in southern Africa during the SAFARI 2000 dry season campaign and a comparison of single scattering albedo estimates from radiometric measurements, J. Geophys. Res.-Atmos., 108, 8477, https://doi.org/10.1029/2002JD002321, 2003.

Ellison, W.: Permittivity of pure water, at standard atmospheric pressure, over the frequency range 0–25 THz and the temperature range 0–100 C, Journal of physical and chemical reference data, 36, 1–18, https://doi.org/10.1063/1.2360986, 2007.

English, S.: Airborne radiometric observations of cloud liquid-water emission at 89 and 157 GHz: Application to retrieval of liquid-water path, Quarterly Journal of the Royal Meteorological Society, 121, 1501–1524, https://doi.org/10.1002/qj.49712152702, 1995.

Formenti, P., D'Anna, B., Flamant, C., Mallet, M., Piketh, S. J., Schepanski, K., Waquet, F., Auriol, F., Brogniez, G., Burnet, F., et al.: The Aerosols, Radiation and Clouds in southern Africa (AEROCLO-sA) field campaign in Namibia: overview, illustrative observations and way forward, Bulletin of the American Meteorological Society, https://doi.org/10.1175/BAMS-D-17-0278.1, 2019.

Francis, P. N., Hocking, J. A., and Saunders, R. W.: Improved diagnosis of low-level cloud from MSG SEVIRI data for assimilation into Met Office limited area models, in: Proceedings of the 2008 EUMETSAT Meteorological Satellite Conference, Darmstadt, 2008.

Hamann, U., Walther, A., Baum, B., Bennartz, R., Bugliaro, L., Derrien, M., Francis, P. N., Heidinger, A., Joro, S., Kniffka, A., Le Gleau, H., Lockhoff, M., Lutz, H. J., Meirink, J. F., Minnis, P., Palikonda, R., Roebeling, R., Thoss, A., Platnick, S., Watts, P., and Wind, G.: Remote sensing of cloud top pressure/height from SEVIRI : analysis of ten current retrieval algorithms, Atmospheric Measurement Techniques, 7, 2839–2867, https://doi.org/10.5194/amt-7-2839-2014, 2014.

Haywood, J. M., Osborne, S. R., and Abel, S. J.: The effect of overlying absorbing aerosol layers on remote sensing retrievals of cloud effective radius and cloud optical depth, Quarterly Journal of the Royal Meteorological Society, 130, 779–800, https://doi.org/10.1256/qj.03.100, https://rmets.onlinelibrary.wiley.com/doi/abs/10.1256/qj.03.100, 2004.

Haywood, J. M., Abel, S. J., Barrett, P. A., Bellouin, N., Blyth, A., Bower, K. N., Brooks, M., Carslaw, K., Che, H., Coe, H., Cotterell, M. I., Crawford, I., Cui, Z., Davies, N., Dingley, B., Field, P., Formenti, P., Gordon, H., de Graaf, M., Herbert, R., Johnson, B., Jones, A. C., Langridge, J. M., Malavelle, F., Partridge, D. G., Peers, F., Redemann, J., Stier, P., Szpek, K., Taylor, J. W., Watson-Parris, D., Wood, R., Wu, H., and Zuidema, P.: Overview: The CLoud-Aerosol-Radiation Interaction and Forcing: Year-2017 (CLARIFY-2017) measurement campaign, Atmos. Chem. Phys. Discuss., https://doi.org/10.5194/acp-2020-729, in review, 2020.

~~Haywood, J. M., S. J. Abel, P. Barrett, N. Bellouin, A. Blyth, K.N. Bower, M. Brooks, K. Carslaw, H. Coe, M. Cotterell, I. Crawford, N. Davies, E. Dingley, P. Field, P. Formenti, H. Gordon, M. de Graaf, R. Herbert, B. Johnson, A.C. Jones, J. Langridge, F. Malavelle, D.G. Partridge, F. Peers, J. Redemann, P. Stier, K. Szpek, J. Taylor, D. Watson-Parris, R. Wood, H.H. Wu, P. Zuidema: Overview of the CLoud-Aerosol-Radiation Interaction and Forcing: Year-2017 (CLARIFY-2017) measurement campaign, in preparation for ACP.~~

Hu, Y., Vaughan, M., Liu, Z., Powell, K., and Rodier, S.: Retrieving optical depths and lidar ratios for transparent layers above opaque water clouds from CALIPSO lidar measurements, IEEE Geoscience and Remote Sensing Letters, 4, 523–526, doi: 10.1109/LGRS.2007.901085, 2007.

Jethva, H., Torres, O., Remer, L. A., and Bhartia, P. K.: A Color Ratio Method for Simultaneous Retrieval of Aerosol and Cloud Optical Thickness of Above-Cloud Absorbing Aerosols From Passive Sensors: Application to MODIS Measurements, IEEE Transactions on Geoscience and Remote Sensing, 51, 3862 – 3870, https://doi.org/10.1109/TGRS.2012.2230008, 2013.

Jethva, H., Torres, O., Waquet, F., Chand, D., and Hu, Y.: How do A-train sensors intercompare in the retrieval of above-cloud aerosol optical depth? A case study-based assessment, Geophysical Research Letters, 41, 186–192, https://doi.org/10.1002/2013GL058405, 2014.

Jethva, H., Torres, O., Remer, L., Redemann, J., Livingston, J., Dunagan, S., Shinozuka, Y., Kacenelenbogen, M., Rosenheimer, M. S., and Spurr, R.: Validating MODIS above-cloud aerosol optical depth retrieved from "color ratio" algorithm using direct measurements made by NASA's airborne AATS and 4STAR sensors, Atmospheric Measurement Techniques, 9, 5053–5062, https://doi.org/10.5194/amt-9- 5053-2016, 2016.

Kacenelenbogen, M. S., Vaughan, M. A., Redemann, J., Young, S. A., Liu, Z., Hu, Y., Omar, A. H., LeBlanc, S., Shinozuka, Y., Livingston, J., Zhang, Q., and Powell, K. A.: Estimations of global shortwave direct aerosol radiative effects above opaque water clouds using a combination of A-Train satellite sensors, Atmos. Chem. Phys., 19, 4933–4962, https://doi.org/10.5194/acp-19-4933-2019, 2019.

Keil, A. and Haywood, J.: Solar radiative forcing by biomass aerosol particles over marine clouds during SAFARI-2000, Journal of Geophysical Research, 108, 8467, https://doi.org/10.1029/2002JD002315, 2003.

Lack, D. A., Richardson, M. S., Law, D., Langridge, J. M., Cappa, C. D., McLaughlin, R. J., and Murphy, D. M.: Aircraft instrument for comprehensive characterization of aerosol optical properties, part 2: black and brown carbon absorption and absorption enhancement measured with photo acoustic spectroscopy, Aerosol science and technology, 46, 555–568, https://doi.org/10.1080/02786826.2011.645955, 2012.

Levy, R. C., Remer, L. A., Tanre, D., Mattoo, S., and Kaufman, Y. J.: Algorithm for remote sensing of tropospheric aerosol over dark targets from MODIS: Collections 005 and 051: Revision 2; Feb 2009, MODIS algorithm theoretical basis document, 2009.

Liu, Q., Weng, F., and English, S. J.: An improved fast microwave water emissivity model, IEEE Transactions on Geoscience and Remote Sensing, 49, 1238–1250, doi: 10.1109/TGRS.2010.2064779, 2010.

~~Liu, Z., Kuehn, R., Vaughan, M., Winker, D., Omar, A., Powell, K., Trepte, C., Hu, Y., and Hostetler, C.: The CALIPSO cloud and aerosol discrimination: Version 3 algorithm and test results, in: 25th International Laser Radar Conference (ILRC), St. Petersburg, Russia, pp. 5–9, 2010b.~~

Magi, B. I. and Hobbs, P. V.: Effects of humidity on aerosols in southern Africa during the biomass burning season, Journal of Geophysical Research: Atmospheres, 108, https://doi.org/10.1029/2002JD002144, https://agupubs.onlinelibrary.wiley.com/doi/abs/10. 1029/2002JD002144, 2003.

Marshak, A. and Davis, A.: 3D radiative transfer in cloudy atmospheres. Springer Science & Business Media, doi: 10.1007/3-540-28519-9, 2005.

Marshak, A., Platnick, S., Várnai, T., Wen, G., and Cahalan, R. F.: Impact of three-dimensional radiative effects on satellite retrievals of cloud droplet sizes, Journal of Geophysical Research: Atmospheres, 111, https://doi.org/10.1029/2005JD006686, 2006.

McClatchey, R. A., Fenn, R. W., Selby, J. A., Volz, F., and Garing, J.: Optical properties of the atmosphere, Tech. rep., Air Force Cambridge Research Labs HANSCOM AFB MA, 1972.

McGrath, A. and Hewison, T.: Measuring the accuracy of MARSS—An airborne microwave radiometer, Journal of Atmospheric and Oceanic Technology, 18, 2003–2012, https://doi.org/10.1175/1520-0426(2001)018<2003:MTAOMA>2.0.CO;2, 2001.

Meirink, J. F., Roebeling, R. A., and Stammes, P.: Inter-calibration of polar imager solar channels using SEVIRI, Atmospheric Measurement Techniques, 6, 2495–2508, https://doi.org/10.5194/amt-6-2495-2013, https://www.atmos-meas-tech.net/6/2495/2013/, 2013.

Meyer, K., Platnick, S., and Zhang, Z.: Simultaneously inferring above-cloud absorbing aerosol optical thickness and underlying liquid phase cloud optical and microphysical properties using MODIS, Journal of Geophysical Research: Atmospheres, 120, 5524–5547, https://doi.org/10.1002/2015JD023128, https://agupubs.onlinelibrary.wiley.com/doi/abs/10.1002/2015JD023128, 2015.

Myhre, G., Samset, B. H., Schulz, M., Balkanski, Y., Bauer, S., Berntsen, T. K., Bian, H., Bellouin, N., Chin, M., Diehl, T., Easter, R. C., Feichter, J., Ghan, S. J., Hauglustaine, D., Iversen, T., Kinne, S., Kirkevåg, A., Lamarque, J.-F., Lin, G., Liu, X., Lund, M. T., Luo, G., Ma, X., van Noije, T., Penner, J. E., Rasch, P. J., Ruiz, A., Seland, Ø., Skeie, R. B., Stier, P., Takemura, T., Tsigaridis, K., Wang, P., Wang, Z., Xu, L., Yu, H., Yu, F., Yoon, J.-H., Zhang, K., Zhang, H., and Zhou, C.: Radiative forcing of the direct aerosol effect from AeroCom Phase II simulations, Atmospheric Chemistry and Physics, 13, 1853–1877, https://doi.org/10.5194/acp-13-1853-2013, https://www.atmos-chem-phys.net/13/1853/2013/, 2013.

Painemal, D. and Zuidema, P.: Assessment of MODIS cloud effective radius and optical thickness retrievals over the Southeast Pacific with VOCALS-REx in situ measurements, Journal of Geophysical Research: Atmospheres, 116, https://doi.org/10.1029/2011JD016155, 2011.

Peers, F., Waquet, F., Cornet, C., Dubuisson, P., Ducos, F., Goloub, P., Szczap, F., Tanré, D., and Thieuleux, F.: Absorption of aerosols above clouds from POLDER/PARASOL measurements and estimation of their direct radiative effect, Atmospheric Chemistry and Physics, 15, 4179–4196, https://doi.org/10.5194/acp-15-4179-2015, 2015.

Peers, F., Francis, P., Fox, C., Abel, S. J., Szpek, K., Cotterell, M. I., Davies, N. W., Langridge, J. M., Meyer, K. G., Platnick, S. E., and Haywood, J. M.: Observation of absorbing aerosols above clouds over the south-east Atlantic Ocean from the geostationary satellite SEVIRI – Part 1: Method description and sensitivity, Atmospheric Chemistry and Physics, 19, 9595–9611, https://doi.org/10.5194/acp-19-9595-2019, 2019.

Pistone, K., Redemann, J., Doherty, S., Zuidema, P., Burton, S., Cairns, B., Cochrane, S., Ferrare, R., Flynn, C., Freitag, S., Howell, S. G., Kacenelenbogen, M., LeBlanc, S., Liu, X., Schmidt, K. S., Sedlacek III, A. J., Segal-Rozenhaimer, M., Shinozuka, Y., Stamnes, S., van Diedenhoven, B., Van Harten, G., and Xu, F.: Intercomparison of biomass burning aerosol optical properties from in situ and remote-sensing instruments in ORACLES-2016, Atmospheric Chemistry and Physics, 19, 9181–9208, https://doi.org/10.5194/acp-19- 9181-2019, 2019.

Platnick, S.: Vertical photon transport in cloud remote sensing problems, Journal of Geophysical Research: Atmospheres, 105, 22 919– 22 935, https://doi.org/10.1029/2000JD900333, 2000.

Platnick, S., King, M. D., Ackerman, S. A., Menzel, W. P., Baum, B. A., Riédi, J. C., and Frey, R. A.: The MODIS cloud products: Algorithms and examples from Terra, IEEE Transactions on Geoscience and Remote Sensing, 41, 459–473, doi: 10.1109/TGRS.2002.808301, 2003.

Platnick, S., Ackerman, S., King, M., Meyer, K., Menzel, W., Holz, R., Baum, B., and Yang, P.: MODIS atmosphere L2 cloud product (06_L2), NASA MODIS Adaptive Processing System, Goddard Space Flight Center, 10, 1–53, 2015.

Platnick, S., Heidinger, A., Ackerman, S. A., Amarasinghe, N., Dutcher, S., Frey, R., Hubanks, P., Li, Y., Marchant, B., Meyer, K. G., Holz, R. E., Walther, A., Wang, C., and Wind, G.: EOS MODIS and SNPP VIIRS Cloud Properties: User Guide for the Climate Data Record Continuity Level-2 Cloud Top and Optical Properties Product (CLDPROP), Tech. rep., NASA Goddard Space Flight Center, 2019.

Redemann, J., Wood, R., Zuidema, P., Doherty, S. J., Luna, B., LeBlanc, S. E., Diamond, M. S., Shinozuka, Y., Chang, I. Y., Ueyama, R., Pfister, L., Ryoo, J., Dobracki, A. N., da Silva, A. M., Longo, K. M., Kacenelenbogen, M. S., Flynn, C. J., Pistone, K., Knox, N. M., Piketh, S. J., Haywood, J. M., Formenti, P., Mallet, M., Stier, P., Ackerman, A. S., Bauer, S. E., Fridlind, A. M., Carmichael, G. R., Saide, P. E., Ferrada, G. A., Howell, S. G., Freitag, S., Cairns, B., Holben, B. N., Knobelspiesse, K. D., Tanelli, S., L'Ecuyer, T. S., Dzambo, A. M., Sy, O. O., McFarquhar, G. M., Poellot, M. R., Gupta, S., O'Brien, J. R., Nenes, A., Kacarab, M. E., Wong, J. P. S., Small-Griswold, J. D., Thornhill, K. L., Noone, D., Podolske, J. R., Schmidt, K. S., Pilewskie, P., Chen, H., Cochrane, S. P., Sedlacek, A. J., Lang, T. J., Stith, E., Segal-Rozenhaimer, M., Ferrare, R. A., Burton, S. P., Hostetler, C. A., Diner, D. J., Platnick, S. E., Myers, J. S., Meyer, K. G., Spangenberg, D. A., Maring, H., and Gao, L.: An overview of the ORACLES (ObseRvations of Aerosols above CLouds and their intEractionS) project: aerosol-cloud-radiation interactions in the Southeast Atlantic basin, Atmos. Chem. Phys. Discuss., https://doi.org/10.5194/acp-2020-449, in review, 2020.

Rodgers, C. D.: Retrieval of atmospheric temperature and composition from remote measurements of thermal radiation, Reviews of Geophysics, 14, 609–624, https://doi.org/10.1029/RG014i004p00609, 1976.

Rosenberg, P. D., Dean, A. R., Williams, P. I., Dorsey, J. R., Minikin, A., Pickering, M. A., and Petzold, A.: Particle sizing calibration with refractive index correction for light scattering optical particle counters and impacts upon PCASP and CDP data collected during the Fennec campaign, Atmospheric Measurement Techniques, 5, 1147–1163, https://doi.org/10.5194/amt-5-1147-2012, https://www. atmos-meas-tech.net/5/1147/2012/, 2012.

Sayer, A. M., Hsu, N., Bettenhausen, C., Lee, J., Redemann, J., Schmid, B., and Shinozuka, Y.: Extending "Deep Blue" aerosol retrieval coverage to cases of absorbing aerosols above clouds: Sensitivity analysis and first case studies, Journal of Geophysical Research: Atmospheres, 121, 4830–4854, https://doi.org/10.1002/2015JD024729, 2016.

Sayer, A. M., Hsu, N. C., Lee, J., Kim, W. V., Burton, S., Fenn, M. A., Ferrare, R. A., Kacenelenbogen, M., LeBlanc, S., Pistone, K., Redemann, J., Segal-Rozenhaimer, M., Shinozuka, Y., and Tsay, S.-C.: Two decades observing smoke above clouds in the south- eastern Atlantic Ocean: Deep Blue algorithm updates and validation with ORACLES field campaign data, Atmospheric Measurement Techniques, 12, 3595–3627, https://doi.org/10.5194/amt-12-3595-2019, https://www.atmos-meas-tech.net/12/3595/2019/, 2019.

Seethala, C., Meirink, J. F., Horváth, A., Bennartz, R., and Roebeling, R.: Evaluating the diurnal cycle of South Atlantic stratocumulus clouds as observed by MSG SEVIRI, Atmospheric Chemistry and Physics, 18, 13 283–13 304, https://doi.org/10.5194/acp-18-13283- 2018, https://www.atmos-chem-phys.net/18/13283/2018/, 2018.

Seinfeld, J. H., Bretherton, C., Carslaw, K. S., Coe, H., DeMott, P. J., Dunlea, E. J., Feingold, G., Ghan, S., Guenther, A. B., Kahn, R., Kraucunas, I., Kreidenweis, S. M., Molina, M., Nenes, A., Penner, J. E., Prather, K., A., Ramanathan, V., Ramaswamy, V., Rasch, P. J., Ravishankara, A. R., Rosenfeld, D., Stephens, G., and Wood., R..: Improving our fundamental understanding of the role of aerosol- cloud interactions in the climate system, Proceedings of the National Academy of Sciences, 113, 5781–5790, https://doi.org/10.1073/pnas.1514043113, 2016.

~~Stephens, G. L.: Radiation profiles in extended water clouds. I: Theory, Journal of the Atmospheric Sciences, 35, 2111–2122, https://doi.org/10.1175/1520-0469(1978)035<2111:RPIEWC>2.0.CO;2, 1978.~~

Szczap, F., Isaka, H., Saute, M., Guillemet, B., and Ioltukhovski, A.: Effective radiative properties of bounded cascade nonabsorbing clouds: Definition of the equivalent homogeneous cloud approximation, Journal of Geophysical Research: Atmospheres, 105, 20 617–20 633, https://doi.org/10.1029/2000JD900146, 2000.

Taylor, J. W., Wu, H., Szpek, K., Bower, K., Crawford, I., Flynn, M. J., Williams, P. I., Dorsey, J., Langridge, J. M., Cotterell, M. I., Fox, C., Davies, N. W., Haywood, J. M., and Coe, H.: Absorption closure in highly aged biomass burning smoke, Atmos. Chem. Phys., 20, 11201–11221, https://doi.org/10.5194/acp-20-11201-2020, 2020.

Torres, O., Jethva, H., and Bhartia, P. K.: Retrieval of Aerosol Optical Depth above Clouds from OMI Observations: Sensitivity Analysis and Case Studies, Journal of the Atmospheric Sciences, 69, 1037–1053, https://doi.org/10.1175/JAS-D-11-0130.1, https://doi.org/10. 1175/JAS-D-11-0130.1, 2012.

Twomey, S.: The influence of pollution on the shortwave albedo of clouds, Journal of the atmospheric sciences, 34, 1149–1152, https://doi.org/10.1175/1520-0469(1977)034<1149:TIOPOT>2.0.CO;2, 1977.

Waquet, F., Peers, F., Ducos, F., Goloub, P., Platnick, S., Riedi, J., Tanré, D., and Thieuleux, F.: Global analysis of aerosol properties above clouds, Geophysical Research Letters, 40, 5809–5814, https://doi.org/10.1002/2013GL057482, https://agupubs.onlinelibrary.wiley.com/doi/abs/10.1002/2013GL057482, 2013.

Wilcox, E. M.: Direct and semi-direct radiative forcing of smoke aerosols over clouds, Atmos. Chem. Phys., 12, 139–149, https://doi.org/10.5194/acp-12-139-2012, 2012.

Wu, H., Taylor, J. W., Szpek, K., Langridge, J. M., Williams, P. I., Flynn, M., Allan, J. D., Abel, S. J., Pitt, J., Cotterell, M. I., Fox, C., Davies, N. W., Haywood, J., and Coe, H.: Vertical variability of the properties of highly aged biomass burning aerosol transported over the southeast Atlantic during CLARIFY-2017, Atmos. Chem. Phys., 20, 12697–12719, https://doi.org/10.5194/acp-20-12697-2020, 2020.

Zeng, S., Cornet, C., Parol, F., Riedi, J., and Thieuleux, F.: A better understanding of cloud optical thickness derived from the passive sensors MODIS/AQUA and POLDER/PARASOL in the A-Train constellation, Atmospheric Chemistry and Physics, 12, 11 245–11 259, https://doi.org/10.5194/acp-12-11245-2012, 2012.

Zhang, J. and Zuidema, P.: The diurnal cycle of the smoky marine boundary layer observed during August in the remote southeast Atlantic, Atmos. Chem. Phys., 19, 14493–14516, https://doi.org/10.5194/acp-19-14493-2019, 2019.

Zhang, Z. and Platnick, S.: An assessment of differences between cloud effective particle radius retrievals for marine water clouds from three MODIS spectral bands, J. Geophys. Res., 116, D20215, doi:10.1029/2011JD016216, 2011.

Zhang, Z., Ackerman, A. S., Feingold, G., Platnick, S., Pincus, R., and Xue, H.: Effects of cloud horizontal inhomogeneity and drizzle on remote sensing of cloud droplet effective radius: Case studies based on large-eddy simulations, Journal of Geophysical Research: Atmospheres, 117, https://doi.org/10.1029/2012JD017655, 2012.

Zhang, Z., Werner, F., Cho, H. M., Wind, G., Platnick, S., Ackerman, A. S., Di Girolamo, L., Marshak, A., and Meyer, K.: A framework based on 2-D Taylor expansion for quantifying the impacts of subpixel reflectance variance and covariance on cloud optical thickness and effective radius retrievals based on the bispectral method, J. Geophys. Res.-Atmos., 121, 7007–7025, https://doi.org/10.1002/2016jd024837, 2016a.

Zhang, Z., Meyer, K., Yu, H., Platnick, S., Colarco, P., Liu, Z., and Oreopoulos, L.: Shortwave direct radiative effects of above-cloud aerosols over global oceans derived from 8 years of CALIOP and MODIS observations, Atmos. Chem. Phys., 16, 2877–2900, https://doi.org/10.5194/acp-16-2877-2016, 2016b.

Zuidema, P., Leon, D., Pazmany, A., and Cadeddu, M.: Aircraft millimeter-wave passive sensing of cloud liquid water and wa- ter vapor during VOCALS-REx, Atmospheric Chemistry and Physics, 12, 355–369, https://doi.org/10.5194/acp-12-355-2012, https: //www.atmos-chem-phys.net/12/355/2012/, 2012.

Zuidema, P., Redemann, J., Haywood, J., Wood, R., Piketh, S., Hipondoka, M., and Formenti, P.: Smoke and clouds above the southeast Atlantic: Upcoming field campaigns probe absorbing aerosol's impact on climate, Bulletin of the American Meteorological Society, 97, 1131–1135, https://doi.org/10.1175/BAMS-D-15-00082.1, 2016.

Zuidema, P., Sedlacek III, A. J., Flynn, C., Springston, S., Delgadillo, R., Zhang, J., Aiken, A. C., Koontz, A., and Muradyan, P.: The Ascension Island boundary layer in the remote southeast Atlantic is often smoky, Geophysical Research Letters, 45, 4456–4465, https://doi.org/10.1002/2017GL076926, 2018.

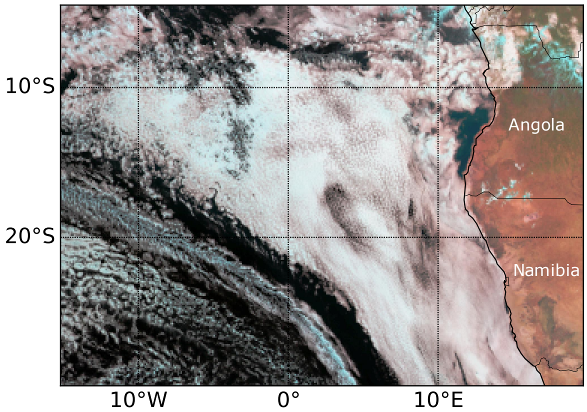

Figure 1: RGB composite obtained from the SEVIRI 0.64 (blue), 0.81 (green) and 1.64 µm (red) channels for the 4th September 2017 at 10:15 UTC over the SEAO.

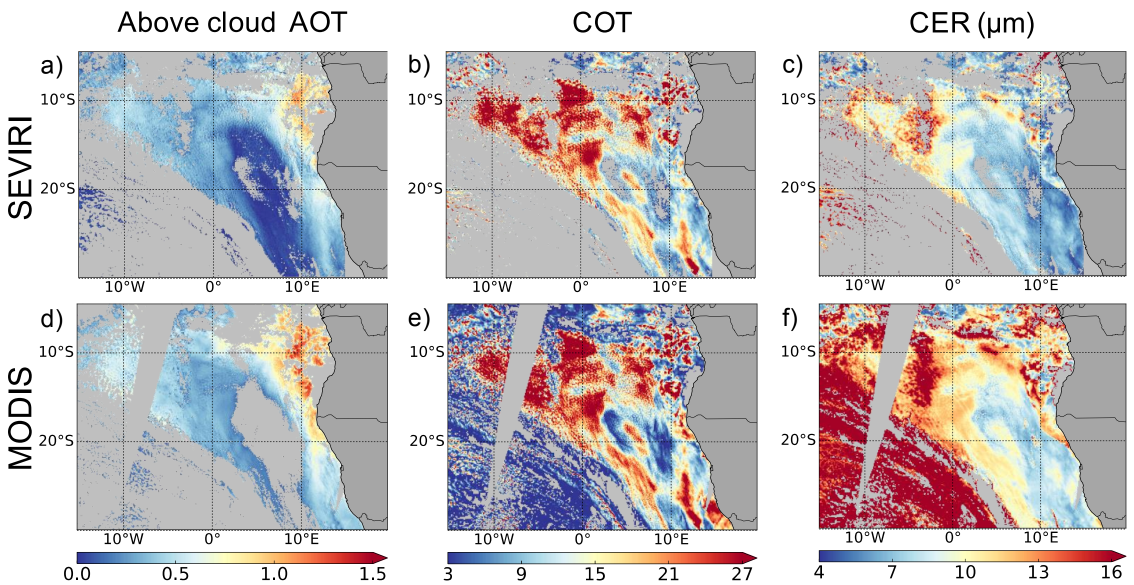

Figure 2: Above cloud AOT at the 0.55 µm optical wavelength and cloud properties retrieved from SEVIRI measurements on the 4th September 2017 at 10:15 UTC over the SEAO (a to c) and corresponding Terra-MODIS observations (10:00 UTC for the east overpass and 11:40 UTC for the west overpass) from the MOD06ACAERO algorithm (d to f).

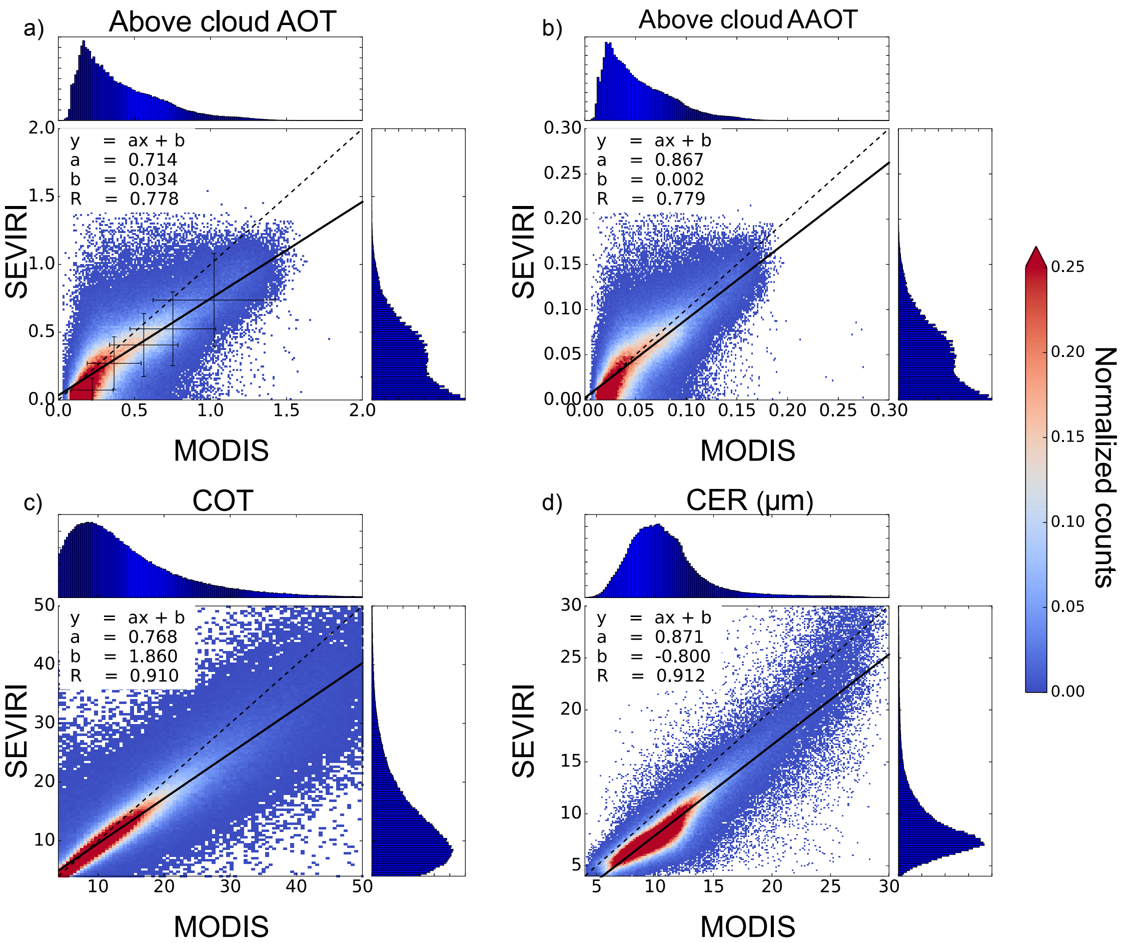

Figure 3: Scatterplots and data distributions for the comparison of the above-cloud AOT (a), AAOT (b), COT(c) and CER (d) from SEVIRI and MODIS MOD06ACAERO retrieval between the 28th August and 5th September 2017 over the area between 0˚N - 30˚S and 20˚W - 15˚E. The solid lines represent the linear regression and the dashed lines are the 1:1 lines. R corresponds to the Pearson's correlation coefficient.

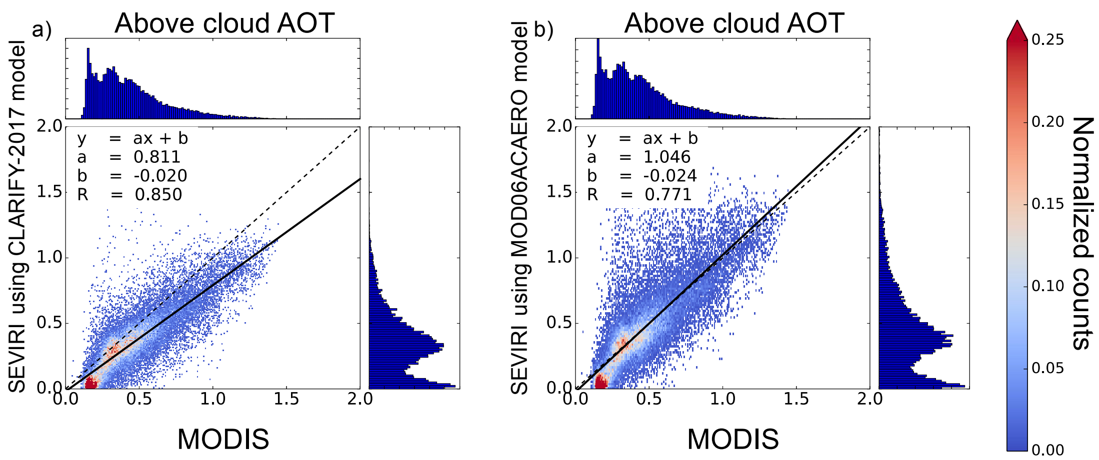

Figure 4: Comparison of the above-cloud AOT retrieved by SEVIRI and MODIS (MOD06ACAERO) in the morning of the 4th September 2017 over the area between 0˚N - 30˚S and 20˚W - 15˚E. The left plot (a) corresponds to the SEVIRI retrieval using the CLARIFY-2017 aerosol model and the right plot (b) shows the SEVIRI retrieval using the same aerosol model as the MODIS retrieval. The solid lines represent the linear regression and the dashed lines are the 1:1 lines. R corresponds to the Pearson's correlation coefficient.

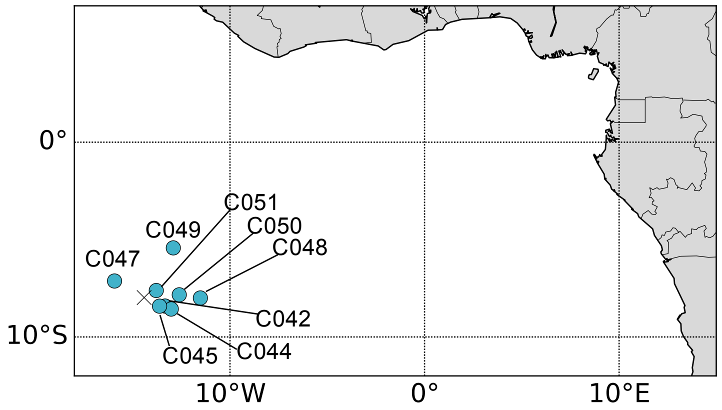

Figure 5: Map showing the geographical location of the dropsonde observations used in section 3. The cross corresponds to Ascension Island.

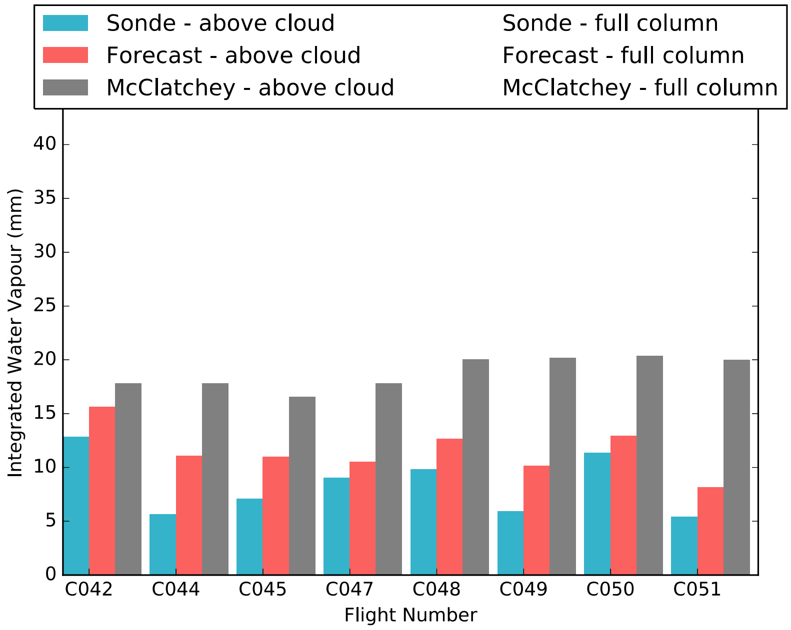

5

Figure 6: Comparison of the water vapour integrated over the full column (lighter shades) and above clouds (darker shades) from the dropsondes, the forecast and the McClatchey tropical atmospheric profile. For the McClatchey and the forecast, the top of the cloud is based on the cloud top height retrieved by SEVIRI.

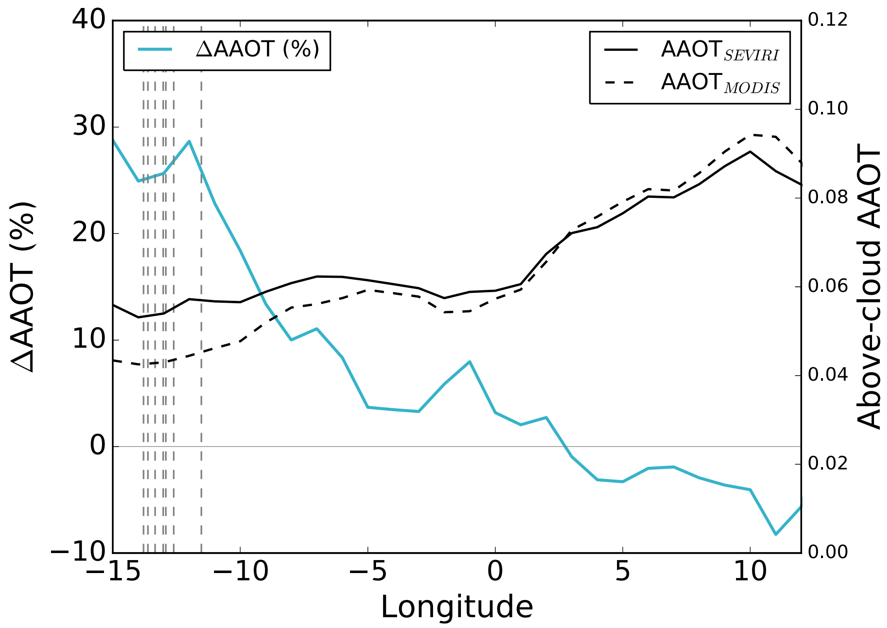

Figure 7: Longitudinal variation of the above-cloud AAOT from SEVIRI (black solid line), MODIS (black dashed line) and the difference ΔAAOT in percentage (blue line) for the data used in Figure 3, removing $AAOT_{SEVIRI}$ lower than 0.03. The dashed vertical lines correspond to the location of the dropsondes used in Figure 6.

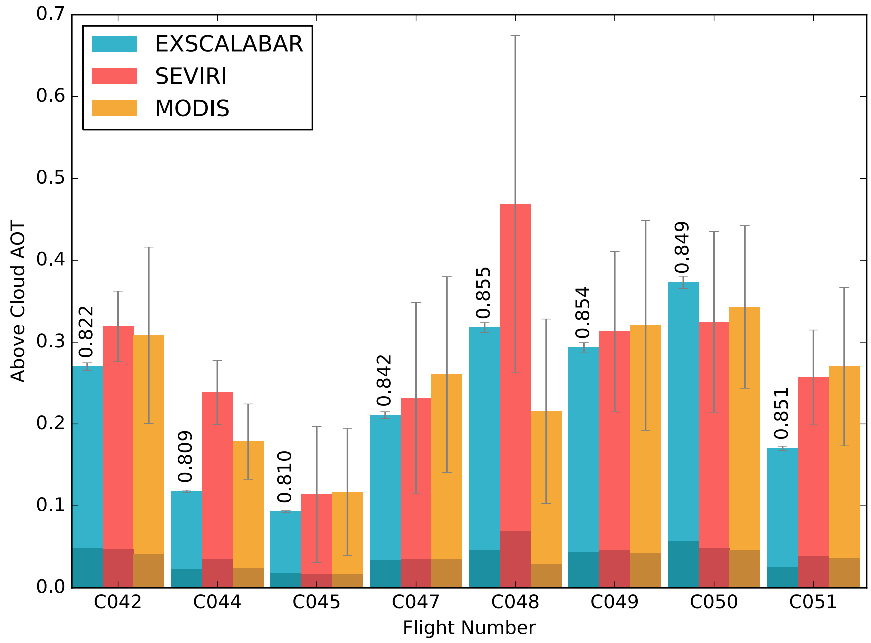

Figure 8: Comparison of the above-cloud AOT (lighter shades) and AAOT (darker shades) retrieved by SEVIRI and MODIS and measured by EXSCALABAR during descent profiles. The error bars represent the uncertainties of the EXSCALABAR measurements and the standard deviation of the satellite product within a 60 km radius around the aircraft measurements for SEVIRI and MODIS. The SSA has been calculated at 0.55 µm from the EXSCALABAR observations and included as an annotation over the EXSCALABAR above-cloud AOT.

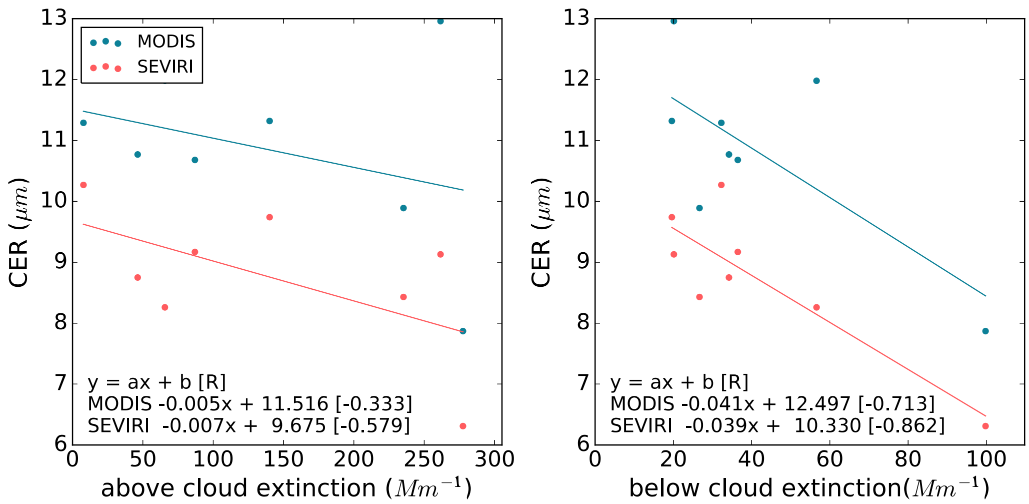

Figure 9: CER (in µm) retrieved by SEVIRI (red) and MODIS (blue) as a function of the dry extinction (in Mm^{-1}) measured by EXSCALABAR at 405 nm and averaged over 100m directly above (a) and below the cloud (b). The linear regression fits are defined by the slope *a*, the intercept *b* and the Pearson's correlation coefficient *R*.

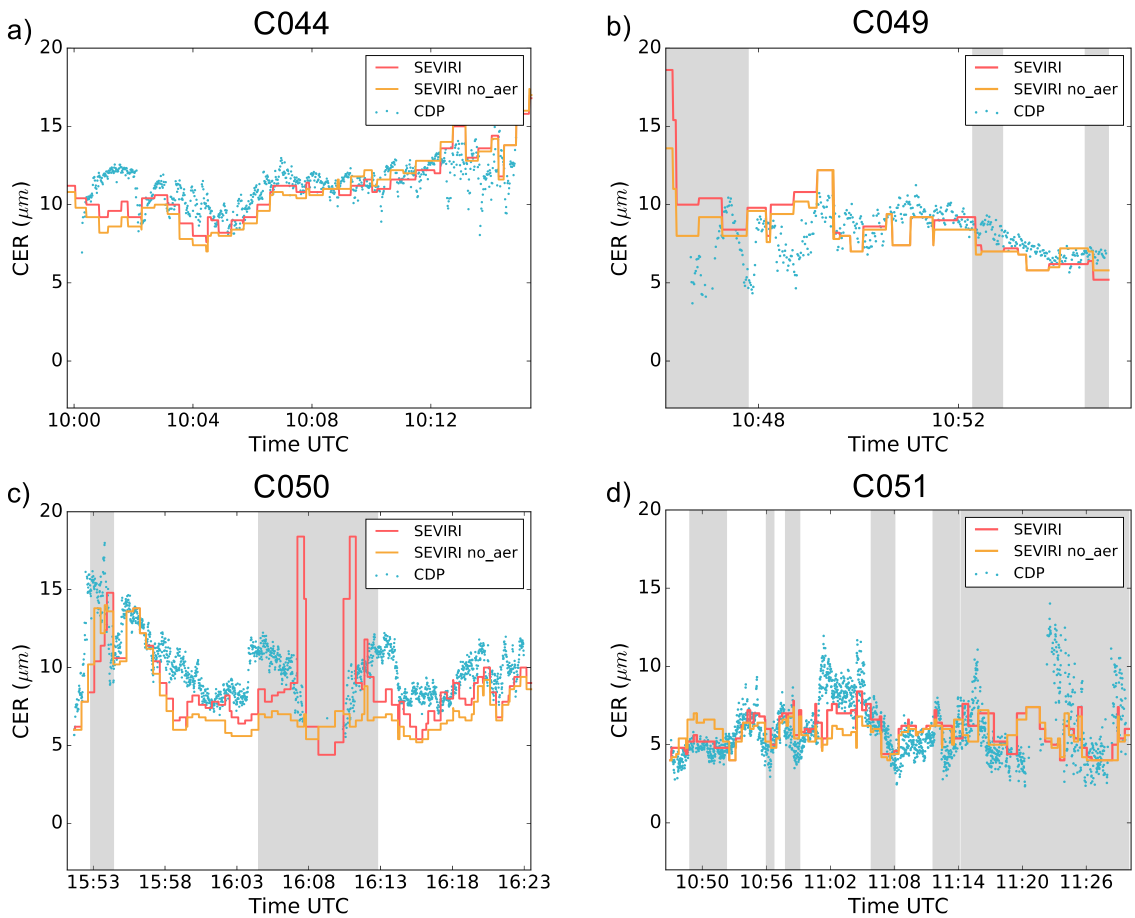

Figure 10: Comparison of the CER measured by the CDP during straight level run through clouds from flight C044 (a), C049 (b), C050 (c) and C051 (d) and the collocated SEVIRI retrievals with and without taking into account the absorption of aerosol above clouds. The grey areas correspond to the SEVIRI pixels that are rejected because of the filters on cloud inhomogeneity, cloud edges and/or unsatisfying fit of the measurements by the forward model.

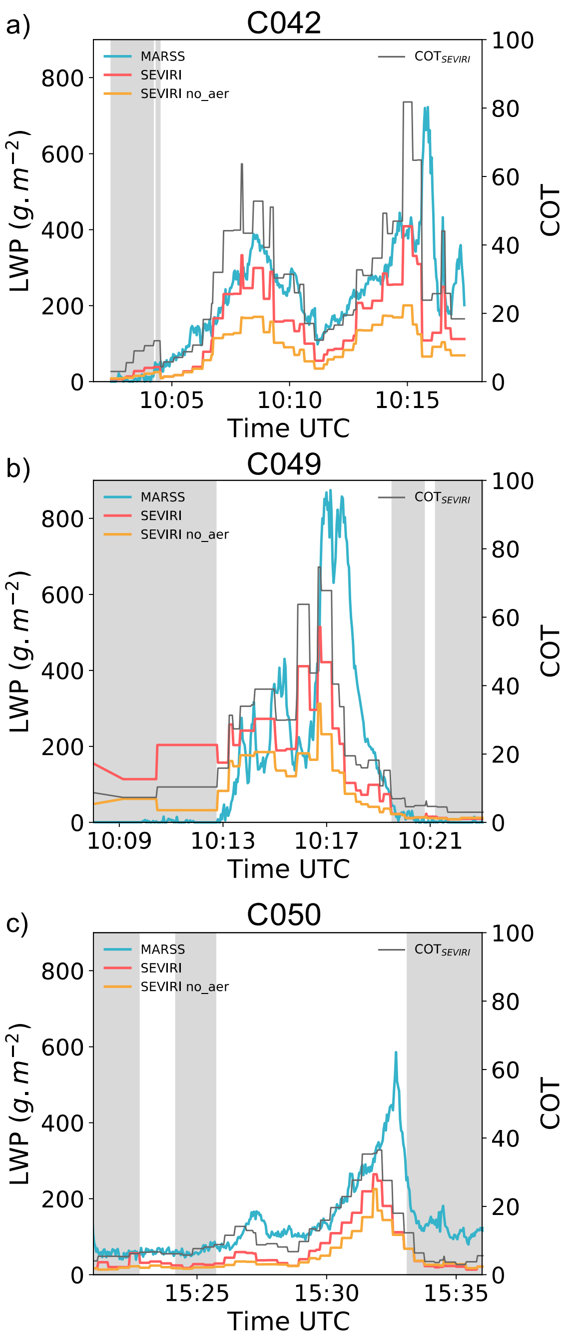

Figure 11: Comparison of the LWP measured from MARSS (blue) during straight level run above the clouds from flight C042 (a), C049 (b) and C050 (c) and collocated LWP from SEVIRI calculated based on the COT and CER retrieved with (red) and without (orange) taking into account the absorption of aerosol above clouds. The COT retrieved by SEVIRI taking into account the overlying aerosols is plotted in black. The grey areas correspond to the SEVIRI pixels that are rejected because of the filters on cloud inhomogeneity, cloud edges and/or unsatisfying fit of the measurements by the forward model.

	SEVIRI			MODIS		
	mean	median	standard deviation	mean	median	standard deviation
AOT	0.329	0.295	0.243	0.413	0.342	0.264
AAOT	0.049	0.044	0.036	0.053	0.045	0.032
COT	13.12	11.26	7.66	14.66	12.30	9.08
CER (µm)	8.79	7.91	3.37	11.01	10.39	3.53

Table 1: Summary statistics of the aerosol and cloud properties retrieved by SEVIRI and MODIS compared in Figure 3.

Flights	C042	C044	C045	C047	C048	C049	C050	C051
ext_{above}	235.27	140.12	7.78	65.67	87.01	46.33	261.61	277.55
ext_{below}	26.68	19.61	32.26	56.60	36.47	34.21	20.13	99.80
CER_{SEVIRI}	8.43	9.74	10.27	8.26	9.17	8.75	9.13	6.31
CER_{MODIS}	9.89	11.32	11.29	11.98	10.68	10.77	12.96	7.87

Table 2: Dry extinction (ext) measured by EXSCALABAR at 405 nm averaged over 100m above and below the cloud (in Mm^{-1}) and collocated CER (in µm) retrieved by SEVIRI and MODIS.

		MARSS	SEVIRI	SEVIRI (no aerosol)
C042	LWP ($g.m^{-2}$)	244.83	191.82	117.03
	COT	-	30.15	18.90
	CER (µm)	-	9.04	8.64
C049	LWP ($g.m^{-2}$)	287.32	250.97	150.02
	COT	-	31.94	19.48
	CER (µm)	-	11.47	10.73
C50	LWP ($g.m^{-2}$)	155.82	88.22	64.66
	COT	-	13.71	10.90
	CER (µm)	-	8.56	7.76

Table 3: Mean LWP observed by MARSS during the straight level run above the clouds and collocated cloud properties retrieved by SEVIRI with and without taking into account the absorption of aerosol above clouds.